Metabolism 181 (2026) 156652

Contents lists available at ScienceDirect

Metabolism

journal homepage: www.journals.elsevier.com/metabolism

Gut-liver metabolic and enterohormonal remodeling drives progression from metabolic dysfunction-associated steatotic liver disease to steatohepatitis☆

Jaclyn A. Rivas [a,1], Alexandria C. Murphy [b,1], Praveena Prasad [b], Mahmoud S. Yahia [b], Siem S. Goitom [a], Aaron S. Romero [a], Crystal Madera Enriquez [a], Brianna B. Maes [a], Prithvi R. Akepati [a], Marcus A. Garcia [a], Fredine T. Lauer [a], Rama R. Gullapalli [c], Kristen M. Gonzales [d], Jessica M. Gross [e], Jing Pu [f], Shuguang Leng [g,h], Julie G. In [a], Melanie R. McReynolds [b,*], Eliseo F. Castillo [a,h,*]

[a] Division of Gastroenterology and Hepatology, Department of Internal Medicine, University of New Mexico Health Sciences, Albuquerque, NM, 87131, USA
[b] Department of Biochemistry and Molecular Biology, Huck Institutes of the Life Sciences, Pennsylvania State University, University Park, PA, 16802, USA
[c] Department of Pathology, University of New Mexico Health Sciences, Albuquerque, NM, 87131, USA
[d] Division of Endocrinology and Metabolism, Department of Internal Medicine, University of New Mexico Health Sciences, Albuquerque, NM, 87131, USA
[e] Clinical and Translational Science Center, University of New Mexico Health Sciences Center, Albuquerque, NM, 87131, USA
[f] Department of Molecular Genetics and Microbiology, University of New Mexico Health Sciences, Albuquerque, NM, 87131, USA
[g] Department of Internal Medicine, University of New Mexico Health Sciences, Albuquerque, NM, 87131, USA
[h] Comprehensive Cancer Center, University of New Mexico Health Sciences, Albuquerque, NM, 87131, USA

ARTICLE INFO

Keywords:
MASLD
MASH
Enteroendocrine hormones
Metabolomics
Lipidomics

ABSTRACT

Background: Metabolic dysfunction-associated steatotic liver disease (MASLD) is a prevalent metabolic liver disease that can progress to metabolic dysfunction-associated steatohepatitis (MASH), a more severe form characterized by inflammation, hepatocyte injury, and fibrosis. Although the gut-liver axis is implicated in disease progression, stage-specific changes in gut-derived metabolites, lipids, and enteroendocrine signaling remain unclear. This study investigated metabolic, lipidomic, and enteroendocrine alterations during MASLD-to-MASH progression.

Methods: Male C57BL/6NTac mice were fed a modified Amylin liver NASH high-fat diet for 16 weeks to induce MASLD or 29 weeks to induce MASH, age-matched chow-fed mice served as controls. Liver, colon, and stool underwent untargeted metabolomics and lipidomics. Plasma hormones and cytokines were measured by multiplex assay and ELISA. Histology, immunofluorescence, disease-signature enrichment, cross-species network analysis, and organoid differentiation assays were used to assess tissue pathology and signaling pathways.

Results: The high-fat diet produced histologically confirmed MASLD and MASH at 16 and 29 weeks, respectively. Cholic acid was elevated across liver, colon, and stool in both stages. MASLD was associated with increased circulating glucagon-like peptide-1, glucose-dependent insulinotropic polypeptide, and peptide YY, which correlated with colonic cholic acid as well as increased colonic TGR5 expression, whereas these changes were absent in MASH. MASH showed broader metabolic and lipid remodeling, elevated tumor necrosis factor and interleukin-6, impaired enteroendocrine differentiation markers, and increased hepatic serotonin colocalized with fibronectin.

Conclusions: MASLD-to-MASH progression involves stage-specific gut-liver metabolic remodeling, loss of enteroendocrine responsiveness, and hepatic serotonergic-fibrotic signaling.

☆ BioRxiv DOI: 10.1101/2025.09.16.676598.

* Corresponding authors at: University of New Mexico, Division of Gastroenterology and Hepatology, Department of Internal Medicine, University of New Mexico Health Sciences Center, Albuquerque, NM, 87131, USA.
E-mail addresses: mcreynolds@psu.edu (M.R. McReynolds), ecastillo@salud.unm.edu (E.F. Castillo).

[1] Authors contributed equally to this paper.

https://doi.org/10.1016/j.metabol.2026.156652
Received 14 October 2025; Accepted 17 May 2026
Available online 20 May 2026

1. Introduction

Metabolic Dysfunction-Associated Steatotic Liver Disease (MASLD) and its more advanced form, Metabolic Dysfunction-Associated Steatohepatitis (MASH), are emerging global health concerns driven by the obesity epidemic [1]. Recent estimates indicate the approximately 30–40% of adults worldwide currently have MASLD with prevalence rising in parallel with obesity and type 2 diabetes [2]. The United States projections suggest further increases in disease burden and associated complications through 2050 [3]. MASLD is characterized by hepatic fat accumulation, while MASH is marked by inflammation, hepatocyte injury, and fibrosis, potentially progressing to cirrhosis and hepatocellular carcinoma [4–7]. Despite the rising incidence of these diseases, the mechanisms driving the progression from simple steatosis (MASLD) to more severe steatohepatitis (MASH) remain poorly understood.

Enteroendocrine cells (EECs), which release hormones such as glucagon-like peptide-1 (GLP-1) and glucose-dependent insulinotropic polypeptide (GIP) to regulate metabolism and liver function, yet their precise role in the progression from MASLD to MASH is still unclear [8–13]. Recent therapeutic advancements have focused on targeting

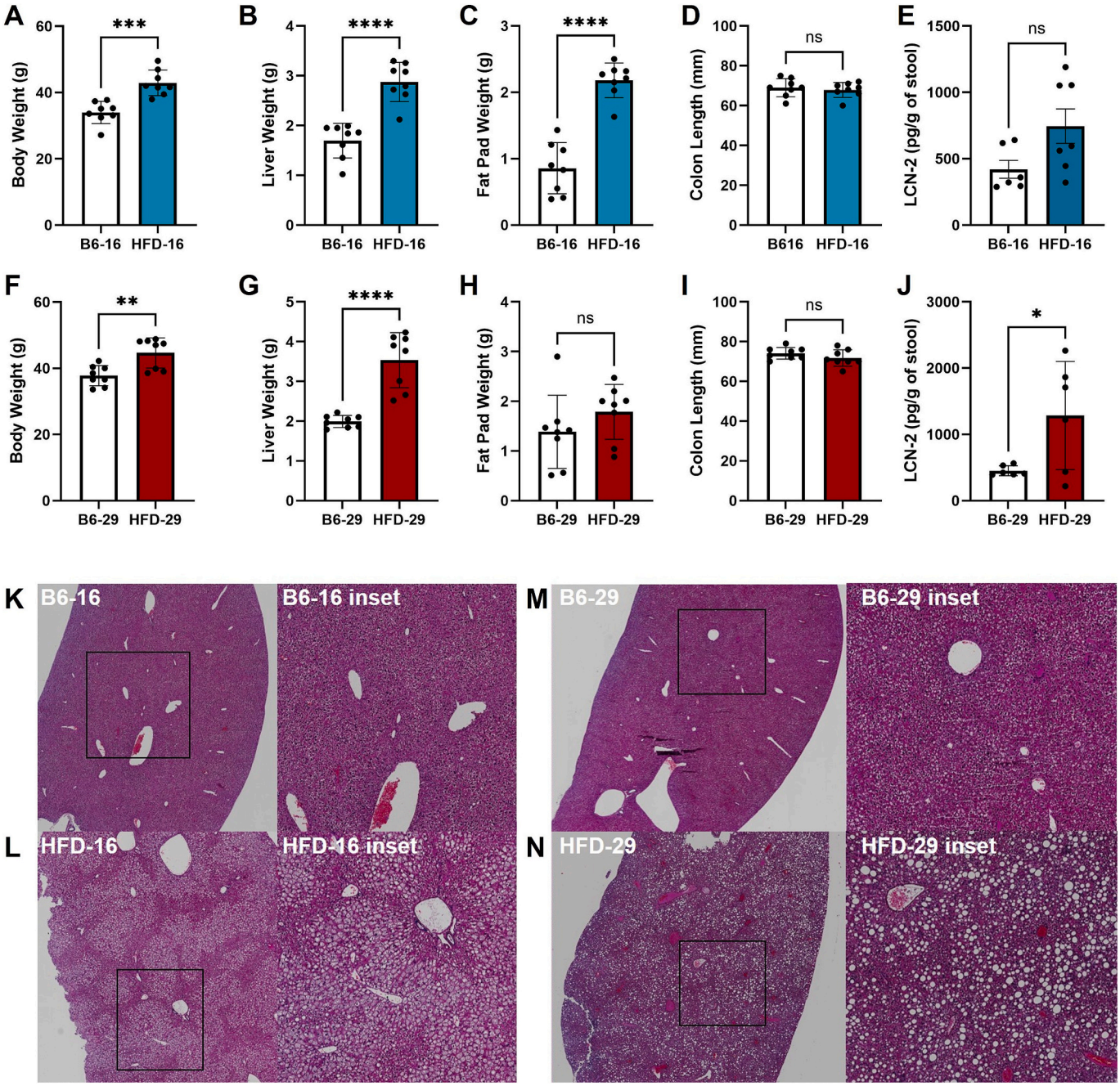

Fig. 1. Gross assessment of diet-induced steatosis. C57BL/6NTac male mice were fed a modified Amylin liver NASH diet starting at 6 weeks of age to induce metabolic dysfunction-associated steatotic liver disease (MASLD) after 16 weeks (HFD-16) or metabolic dysfunction-associated steatohepatitis (MASH) after 29 weeks (HFD-29). Age-matched control mice (B6–16 and B6–29) were maintained on a standard NIH-31 M chow diet. (A-E) Endpoint measurements in B6–16 vs HFD-16: (**A**) body weight, (**B**) liver weight, (**C**) fat pad weight, (**D**) colon length, and (**E**) fecal lipocalin-2 (LCN-2) levels. (F-J) Endpoint measurements in B6–29 vs HFD-29: (**F**) body weight, (**G**) liver weight, (**H**) fat pad weight, (**I**) colon length, and (**J**) fecal LCN-2 levels. (K-N) Representative H&E-stained liver sections from (**K**) B6–16, (**L**) HFD-16, (**M**) B6–29 and (**N**) HFD-29; histopathologic scoring summarized in Table S1. $n = 8$ mice per group. Data analyzed using Student's *t*-test. $^{*}P < 0.05$, $^{**}P < 0.005$, $^{***}P < 0.0005$, $^{****}P < 0.0001$.

metabolic regulation and liver inflammation, with GLP-1 receptor agonists, such as liraglutide and semaglutide, emerging as promising treatments. These therapies have demonstrated improved insulin sensitivity, reduce hepatic steatosis, and attenuate liver inflammation in both MASLD and MASH [14–19]. This success has translated clinically, as GLP-1 and GIP receptor dual agonists, like tirzepatide, have shown the potential to reduce hepatic fat accumulation and inflammation while improving insulin sensitivity [20,21].

Other enteroendocrine hormones, such as serotonin (5-HT) produced by enterochromaffin cells (a subtype of EECs) [22,23], have also emerged as an important signaling molecule in peripheral organs, including the gut and liver. Elevated intestinal and circulating 5-HT levels have been linked to liver fibrosis in chronic liver diseases, suggesting that 5-HT may contribute to the progression of MASH [24–26]. In addition to fibrosis, peripheral 5-HT can influence glucose and lipid metabolism, gut motility, EEC feedback, indicating a multifaceted role in metabolism and liver disease [27–29]. Despite these therapeutic advancements of these agents and the potential of some hormones to influence disease progression, the exact mechanisms particularly those involving enteroendocrine cell function and hormone release in fatty liver disease progression, remain incompletely understood.

The gut-liver axis, the bidirectional communication between the gut and liver, plays a critical role in fatty liver disease progression. This study aims to investigate the metabolic and hormonal changes that occur in the gut and liver during the progression from MASLD to MASH, with a particular focus on EECs. By employing metabolomic and lipidomic profiling, organoid and histological analysis, we found changes in hormones, lipids and metabolites that may drive the progression from MASLD to MASH.

2. Results

2.1. Induction of MASLD and MASH with a modified amylin liver NASH diet

Diet-induced steatosis was established by feeding C57BL/6NTac male mice a modified amylin liver NASH diet (described in methods and herein referred to as high-fat diet, HFD) [30,31], which substitutes palm oil for trans fats to mimic the absence of trans fat in the human diet. Starting at 6 weeks of age, mice were put on the HFD for 16 weeks to establish MASLD (HFD-16) and 29 weeks to establish MASH (HFD-29). Age-matched male mice (B6–16 or B6–29) were fed the NIH-31 M chow diet to serve as a control group. As expected, mice on the HFD showed increased body weights (Fig. 1A, F) and liver weights (Fig. 1B, G) compared to the age-matched controls. Histological analysis of the liver from HFD-16 mice revealed steatosis (Table S1 and Fig. 1K, L), consistent with the development of MASLD. Livers from HFD-29 mice showed more severe pathology, including a higher grade of steatosis, inflammation, hepatocellular hypertrophy, and fibrosis (Table S1 and Fig. 1M, N), indicative of the progression to MASH. Inguinal fat pad weights were increased in HFD-16 compared to controls (Fig. 1C), although there were no significant weight differences in the inguinal fat pads when comparing HFD-29 and B6–29 (Fig. 1H). There were no observed differences in colon length between groups (Fig. 1D, I). Histological assessment also showed no intestinal inflammation in HFD-16 or HFD-29 mice compared to age-matched controls (Table S2 and Supplemental Fig. 1 A-D). Stool analysis for lipocalin-2 (LCN-2), a marker of intestinal inflammation [32,33], showed no significant differences between HFD-16 and B6–16 mice (Fig. 1E), but showed an increase in HFD-29 mice (Fig. 1J). LCN-2 is a sensitive non-invasive marker of intestinal inflammation that increases even in the absence of clear histological signs of inflammation [34].

2.2. Metabolic profiles of the liver, colon, and stool from the MASLD mice

To map out metabolomic changes occurring between the gut and liver, untargeted metabolomics was performed on the liver and colon tissue and the stool collected from the colonic lumen across all groups. Key differences are summarized in Table S3. Metabolomics revealed significant alterations in the liver, colon, and stool of mice on an HFD compared to age-matched controls on a normal diet. For the HFD-16 group, several trends emerged in the data. In the colon (Fig. 2A), key metabolites like cholic acid, methylnicotinamide, and N-Me-2PY were significantly increased, while D-Phenyllactic acid, indole-3-ethanol, and other amino acid-related metabolites were significantly decreased. Volcano plots for the liver (Fig. 2C) show metabolites such as cholic acid, nicotinamide, and sucrose were significantly increased, while metabolites including fumarate, indole-3-ethanol, and retinal were notably decreased. In stool samples, metabolites such as cholic acid, cytidine, and 2-PY were significantly elevated, while kynurenic acid, melatonin, and sucrose were reduced (Supplementary Fig. 3A). Overall, the HFD-16 group exhibited notable disruptions in bile acid metabolism, amino acid homeostasis, and energy-related metabolites.

To further characterize the alterations in metabolites, pathway enrichment analysis was performed using the RaMP-DB (Relational database of Metabolomic Pathways) multi-sourced integrated database using multiple disease and pathway enrichment databases [35]. Metabolite enrichment analysis using RaMP-DB revealed significant pathway-level alterations in the colons of HFD-fed mice (Fig. 2B). The top enriched pathways included the glycerol phosphate shuttle, neurotransmitter-related signaling (e.g., GABA receptor signaling, transmission across chemical synapses, and the neuronal system), and amino acid metabolism (e.g., aspartate, folate, and lysine degradation) showing a HFD induces a broad metabolic reprogramming in colonic tissues, with potential impacts on host-microbiome interactions and epithelial signaling networks. To assess disease relevance, mouse colonic metabolites were matched to known human fecal or blood metabolite disease signatures, providing translational context by linking metabolic changes to gastrointestinal, hepatic, and systemic disease phenotypes. Analysis of our HFD-16 metabolites to the fecal signature revealed significant overlap with metabolites associated with colorectal cancer, Crohn's disease, ulcerative colitis, and irritable bowel syndrome, as well as inflammatory conditions such as ankylosing spondylitis and rheumatoid arthritis (Supplementary Fig. 2A). Similarly, blood metabolite signature mapping revealed associations with cirrhosis, colorectal cancer, primary biliary cirrhosis, Alzheimer's disease, and peroxisomal disorders (Supplementary Fig. 2B).

For the liver, pathway enrichment analysis using RaMP-DB revealed strong signatures of liver-specific metabolic processes, including bile acid metabolism, alcohol degradation, vitamin A metabolism, branched-chain and aromatic amino acid metabolism, fatty acid oxidation, and urea cycle pathways (Fig. 2D), all of which are central hepatic functions. Correspondingly, the fecal metabolite disease signature was enriched for obesity and several gut-related conditions: ulcerative colitis, Crohn's disease and celiac disease, as well as inflammatory conditions such as ankylosing spondylitis and rheumatoid arthritis (Supplementary Fig. 2C). The blood metabolite disease signature further reinforced this association, with significant enrichment for obesity, adrenoleukodystrophy, peroxisomal biogenesis defect, and D-bifunctional protein deficiency (Supplementary Fig. 2D).

Metabolomic profiling of stool samples from mice with MASLD revealed extensive alterations in host and microbial metabolism, with pronounced enrichment of pathways linked to lipid signaling, neurotransmission, and inflammation (Supplementary Fig. 3). RaMP-DB pathway analysis identified strong enrichment for tryptophan metabolism and its catabolic pathways leading to NAD^+ (nicotinamide adenine dinucleotide) biosynthesis, as well as the kynurenine pathway (Supplementary Fig. 3B). Additional pathways included glycosphingolipid metabolism, vitamin C metabolism, and eicosanoid synthesis pointing to alterations in lipid mediator production and oxidative stress responses. Notably, pathways involving G protein-coupled receptor (GPCR) signaling, neurotransmitter release, and gene expression

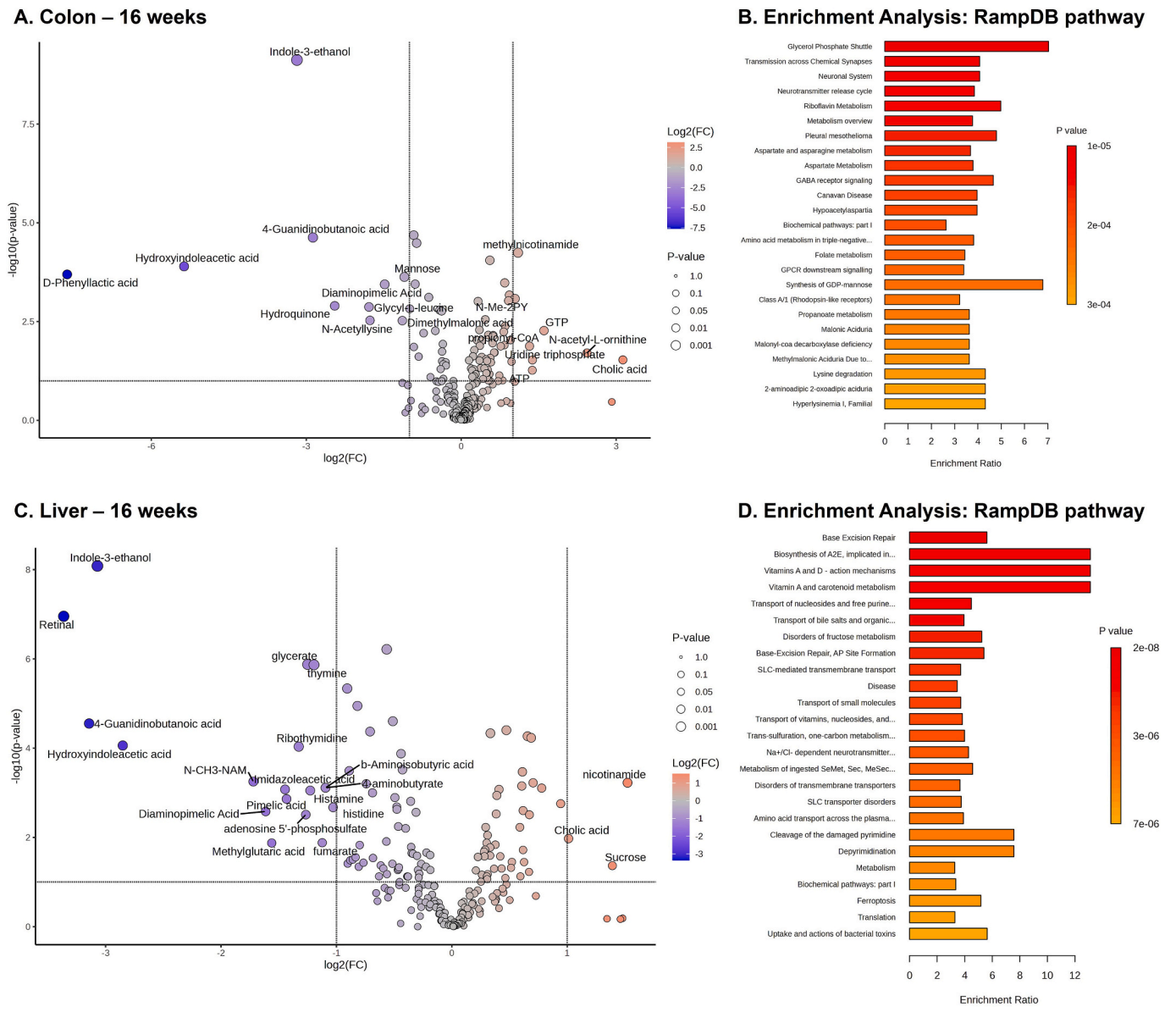

Fig. 2. Metabolomic alterations in the colon and liver of HFD-fed mice at 16 weeks. (**A**, **C**) Volcano plots show significantly altered metabolites in the colon (**A**) and liver (**C**) of mice fed a high-fat diet (HFD-16) compared to age-matched controls on a normal chow diet. Log_2 fold change (x-axis) is plotted against $-log_{10}$ (*p*-value) (y-axis), with dot size indicating significance level and color indicating directionality of change. (**B**, **D**) Metabolite enrichment analysis using RaMP-DB highlights pathway-level changes in colon (**B**) and liver (**D**) metabolomes. Color denotes p-value, and bar length indicates enrichment ratio.

regulation were also enriched, highlighting a potential gut-brain axis signaling. Disease signature analysis of fecal metabolites further supported our colon and liver findings, showing enrichment for gastrointestinal and inflammatory conditions, including ulcerative colitis, Crohn's disease, and diverticular disease, alongside liver conditions like nonalcoholic fatty liver disease (Supplementary Fig. 3C). Complementary analysis of blood metabolite signatures revealed links to diabetes mellitus type 2 and infantile liver failure syndrome 2 as well as systemic metabolic disturbances, particularly in pathways associated with mitochondrial function and lipid oxidation, as evidenced by enrichment for disorders such as 3-hydroxy-3-methylglutaryl-CoA lyase deficiency (Supplementary Fig. 3D). Together, these data reveal that early-stage MASLD is characterized by coordinated metabolic reprogramming across the gut-liver axis, with disruptions in bile acid and amino acid metabolism, microbial signaling, and lipid homeostasis that align with human gastrointestinal, hepatic, and systemic disease signatures.

2.3. Cross-species network analysis reveals conserved metabolic interaction architecture between mouse MASLD and human systems

To assess the translational relevance of the dysregulated liver metabolome identified in our MASLD model, we performed a cross-species network analysis comparing mouse and human metabolite-gene interaction architectures. Fifty-four metabolites significantly altered in MASLD livers were mapped to curated metabolite-protein interaction databases separately using mouse and human genome annotations [36,37]. Network reconstruction revealed a highly conserved interaction landscape, with 88.6% overlap between mouse and human metabolite-associated gene/protein interactions (Fig. 3A,B). Only 5.6% and 5.7% of interactions were uniquely associated with mouse or human databases, respectively. To determine whether these species-specific components altered biological interpretation, we performed KEGG pathway enrichment analysis under two conditions: (1) shared + mouse-unique interactions and (2) shared + human-unique interactions.

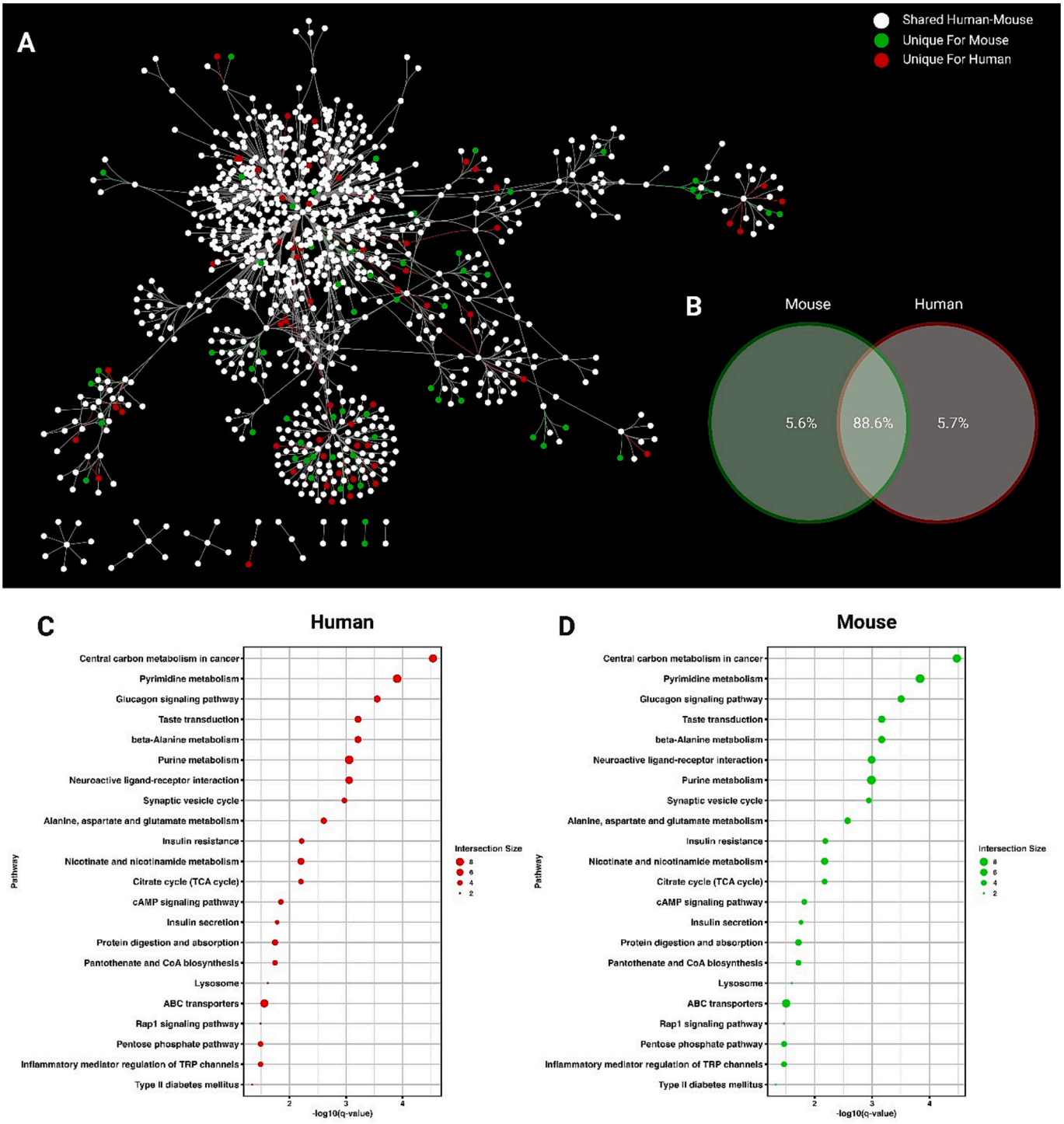

Fig. 3. Cross-species conservation of metabolite-gene interaction networks in the liver of MASLD mice. (**A**) Network representation of metabolite-associated gene/protein interactions derived from 54 dysregulated liver metabolites identified in MASLD. Nodes represent genes/proteins and metabolites; edges represent curated metabolite-gene interactions. White nodes indicate shared human-mouse interactions, green nodes indicate mouse-specific interactions, and red nodes indicate human-specific interactions. (**B**) Venn diagram summarizing overlap between mouse and human interaction networks, demonstrating 88.6% shared interactions, with 5.6% mouse-specific and 5.7% human-specific components. (**C**) KEGG pathway enrichment analysis of the human interaction network (shared + human-unique interactions). Dot size represents intersection size; x-axis shows -log10(q-value). (**D**) KEGG pathway enrichment analysis of the mouse interaction network (shared + mouse-unique interactions). Pathway enrichment profiles were highly concordant between species, indicating conservation of pathway-level metabolic architecture. (For interpretation of the references to color in this figure legend, the reader is referred to the web version of this article.)

Remarkably, pathway enrichment profiles were highly concordant between species (Fig. 3C,D). Core pathways central to MASLD pathophysiology including central carbon metabolism, amino acid metabolism, purine and pyrimidine metabolism, mitochondrial function (citrate cycle), bile acid-associated signaling, glucagon signaling, and energy homeostasis were consistently enriched in both networks. These findings demonstrate that although a small fraction of metabolite interactions exhibit species specificity, the underlying metabolic

interaction architecture and pathway-level biology are strongly conserved between mouse and human systems, supporting the translational relevance of our MASLD metabolomic signatures.

2.4. Metabolic profiles of the liver, colon, and stool from the MASH mice

For the HFD-29 group, the metabolic changes became more pronounced, reflecting the progression from MASLD to MASH. In the colon, key metabolites including cholic acid, glycerate, and *N*-acetyl-L-proline were significantly elevated, while butyric acid, D-Phenyllactic acid, and hydroquinone were some of the metabolites reduced (Fig. 4A). While no intestinal inflammation was observed by histology (Supplementary Fig. 1), the metabolic alterations suggest potential shifts in gut microbial activity and metabolism in response to the prolonged high-fat diet exposure. In the liver, metabolites such as cholic acid, cyclic AMP, and O-phosphoethanolamine were significantly increased, while metabolites like 4-Guanidinobutanoic acid, indole-3-ethanol, and pimelic acid were significantly decreased (Fig. 4C). In stool samples, cholic acid, 2-PY, and leucine were significantly elevated, while metabolites like glucose, kynurenic acid, and melatonin were reduced (Supplementary Fig. 5A).

Pathway and disease enrichment analysis on metabolites derived from colon tissue using RaMP-DB, along with corresponding fecal and blood metabolite signatures were also assessed in MASH mice. RaMP-DB analysis revealed significant enrichment in pathways related to fatty acid biosynthesis, intestinal saccharidase deficiencies, benzene metabolism, and melatonin metabolism, indicating broad disruption of lipid processing, intestinal enzymatic activity, and host-microbe signaling pathways (Fig. 4B). Fecal metabolite signatures were enriched for disease phenotypes associated with intestinal and systemic inflammation, including *Clostridium difficile* infection, sepsis, colorectal cancer, and various enteric infections, highlighting the impact of MASH on gut microbiota-derived metabolism and intestinal barrier integrity (Supplementary Fig. 4A). Disease enrichment analysis of blood metabolites from colon of the MASH mice revealed rare peroxisomal and mitochondrial disorders, including D-bifunctional protein deficiency, peroxisomal biogenesis defects, and adrenoleukodystrophy

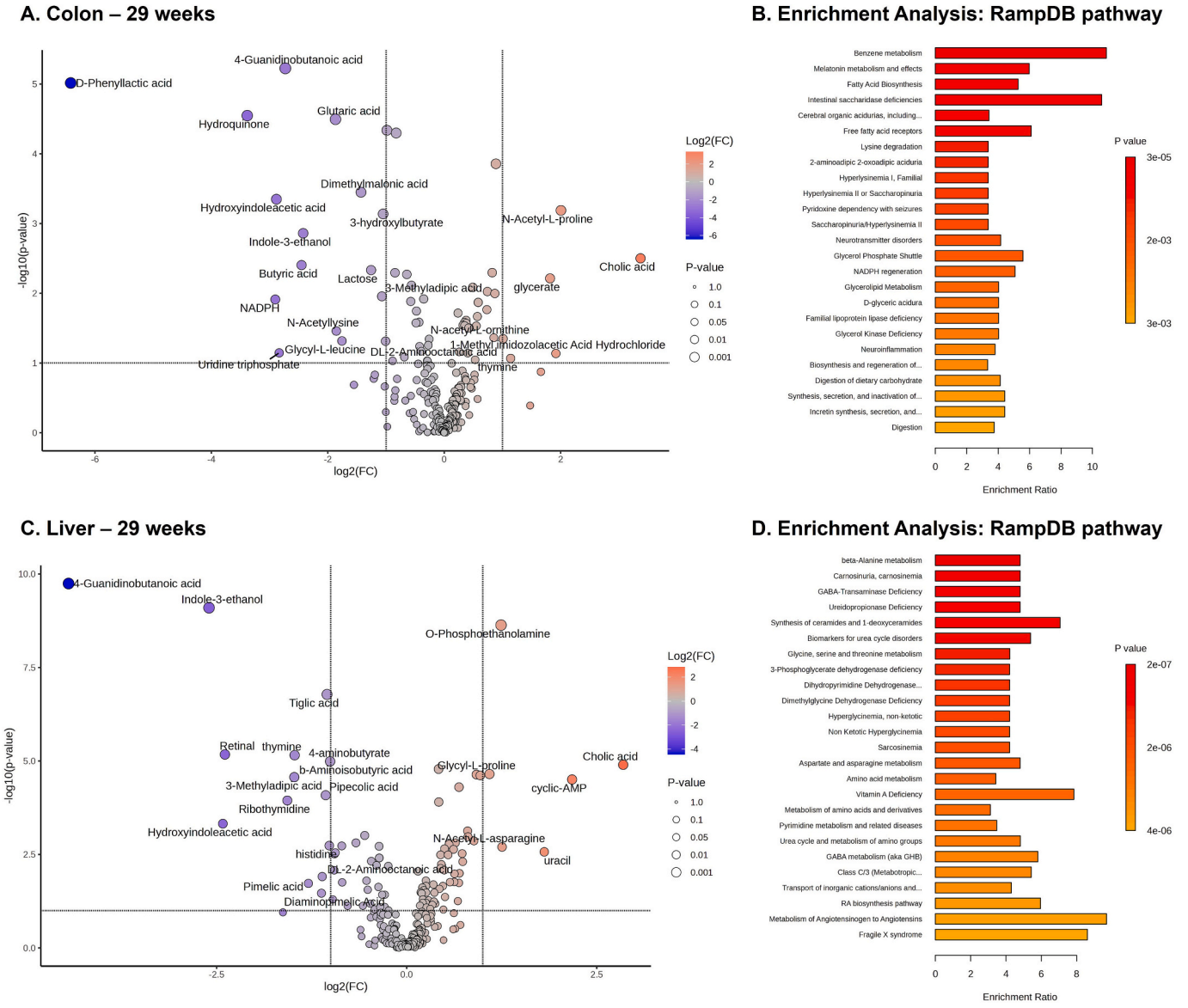

Fig. 4. Metabolomic alterations in the colon and liver of HFD-fed mice at 29 weeks. (**A**, **C**) Volcano plots show significantly altered metabolites in the colon (**A**) and liver (**C**) of mice fed a high-fat diet (HFD-29) compared to age-matched controls on a normal chow diet. Log_2 fold change (x-axis) is plotted against $-log_{10}$ (p-value) (y-axis), with dot size indicating significance level and color indicating directionality of change. (**B**, **D**) Metabolite enrichment analysis using RaMP-DB highlights pathway-level changes in colon (**B**) and liver (**D**) metabolomes. Color denotes p-value, and bar length indicates enrichment ratio.

(Supplementary Fig. 4B). These disorders are characterized by impaired fatty acid oxidation, disrupted lipid homeostasis, and bile acid metabolism abnormalities, consistent with the systemic metabolic stress observed in MASH.

In the liver, RaMP-DB pathway enrichment analysis highlighted significant perturbations in beta-alanine metabolism, carnosinuria/carnosinemia, and deficiencies related to GABA-transaminase and ureidopropionase (Fig. 4D). Additional enriched pathways included the synthesis of ceramides and 1-deoxyceramides, the urea cycle, and broader amino acid metabolic networks. Notably, pathways involved in the metabolism of angiotensinogen and the retinoic acid biosynthesis pathway were also significantly enriched, mirroring findings observed

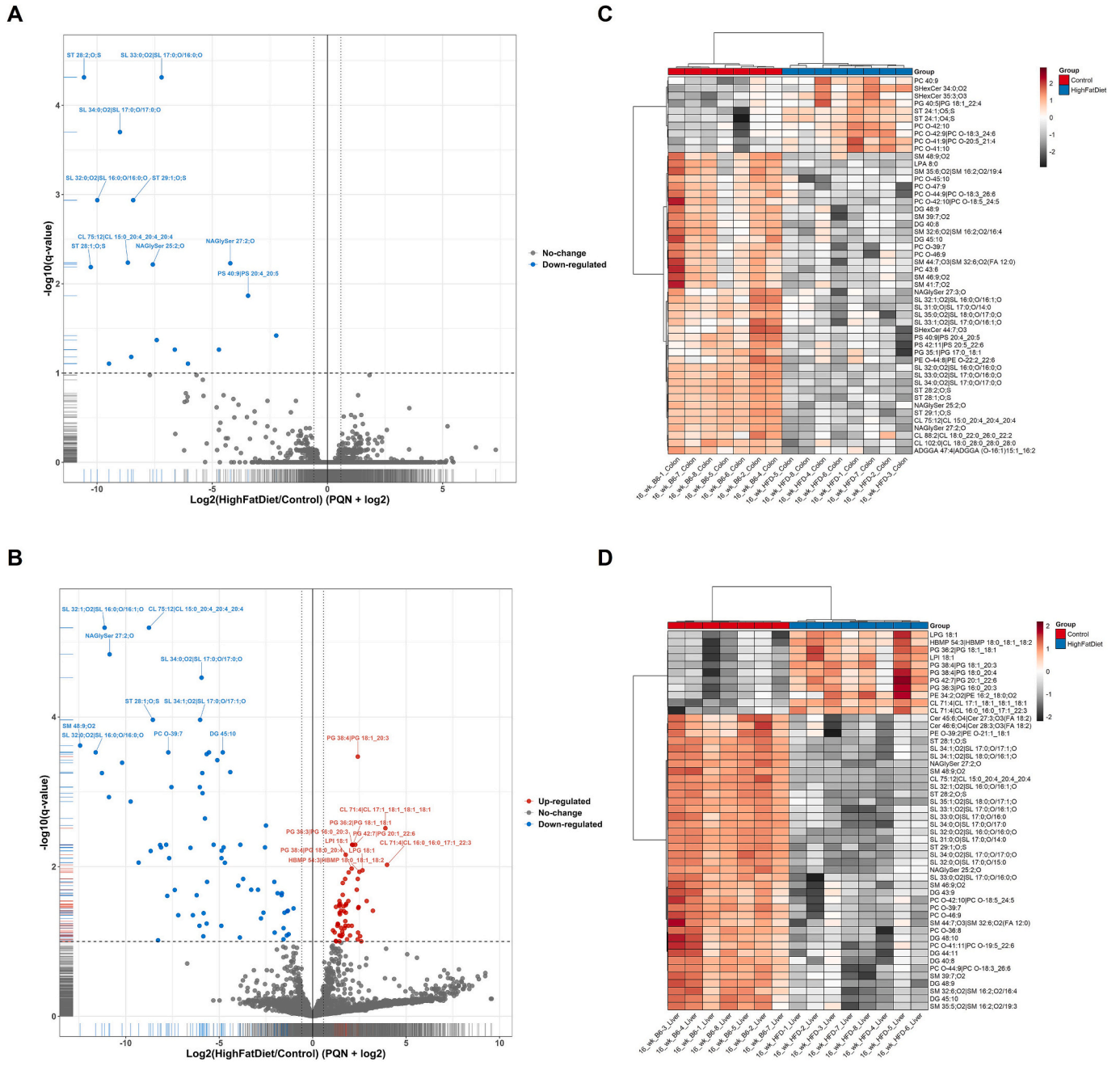

Fig. 5. Lipidomic alterations in the colon and liver of HFD-fed mice at 16 weeks. Red dots show significantly upregulated and blue dots show significantly downregulated lipid class members, grey dots show no change. (Nomenclature- Lipid member name Chain length: unsaturation). (**A**) The volcano plot shows the significantly altered individual members from specific lipid classes with chain length number and unsaturation in the colon of HFD-fed mice (HFD-16), with age-matched controls on normal chow diet as the reference based on log2-fold change and FDR $\leq$ 0.10 (positive and negative ionization modes combined). (**B**) The volcano plot shows the significantly altered individual members from specific lipid classes with chain length number and unsaturation in the liver of HFD-fed mice (HFD-16), with age-matched controls on normal chow diet as the reference based on log2-fold change and FDR $\leq$ 0.10 (positive and negative ionization modes combined). (**C**) This heat map shows top 50 quantitatively altered individual lipid members from specific classes with chain length number and unsaturation in the colon of HFD-fed mice (HFD-16), with age-matched controls on normal chow diet as the reference with sample and feature clustering. Features were ranked based on area. (**D**) This heat map shows top 50 quantitatively altered individual lipid members from specific classes with chain length number and unsaturation in the liver of HFD-fed mice (HFD-16), with age-matched controls on normal chow diet as the reference with sample and feature clustering. Features were ranked based on area. Table S4 details lipid abbreviation. (For interpretation of the references to color in this figure legend, the reader is referred to the web version of this article.)

in the colon dataset and suggesting systemic metabolic involvement. The fecal metabolite disease signature from these liver-targeted metabolites was dominated by gastrointestinal and inflammatory diseases (Supplementary Fig. 4C). Top enrichments included Crohn's disease, ulcerative colitis, and colorectal cancer, along with recurrent *Clostridium difficile* infection and irritable bowel syndrome. Interestingly, signatures for neurological and systemic conditions such as autism and myalgic encephalomyelitis were also present, further supporting the hypothesis of a gut-liver-brain axis playing a role in metabolic regulation and disease susceptibility. Mapping liver metabolites to the blood metabolite disease signature reflected a spectrum of liver-related and systemic conditions (Supplementary Fig. 4D). Cirrhosis was an enriched disease signature, accompanied by diseases such as cystic fibrosis, primary biliary cirrhosis, and uremia were prominent, indicating disruption of hepatobiliary and renal metabolic functions. Neurodegenerative and neuropsychiatric conditions, including Alzheimer's disease and schizophrenia, were also enriched, suggesting broader systemic effects.

For the stool, metabolite profile of MASH mice revealed a distinct disease and pathway enrichment signature indicative of systemic metabolic dysfunction and gut-associated disorders. Enrichment analysis using RaMP-DB showed strong associations with pathways involved in neurotransmitter metabolism, including 5-HT, tryptophan, and kynurenine metabolism, as well as melatonin metabolism and glycosphingolipid metabolism (Supplementary Fig. 5B). Feces disease signature analysis revealed significant enrichment in conditions related to gut inflammation and dysbiosis, including ulcerative colitis, Crohn's disease, *Clostridium difficile* infection, and colorectal cancer (Supplementary Fig. 5C). Additionally, immune-related conditions such as sepsis and iron deficiency further underscore the inflammatory and immunometabolic disturbances linked with MASH. In comparison, the blood-derived metabolite signature highlighted metabolic disorders including NAD deficiency, infantile liver failure syndrome, and congenital adrenal hyperplasia, with strong enrichment in mitochondrial and peroxisomal dysfunction pathways (Supplementary Fig. 5D). Collectively, these data demonstrate that MASH is characterized by extensive metabolic dysregulation across the gut-liver axis, involving disrupted lipid and amino acid metabolism, neurotransmitter pathways, and systemic metabolic stress linked to mitochondrial and peroxisomal dysfunction, with metabolite signatures associated with intestinal barrier impairment, inflammation, and neuroimmune disorders.

2.5. Tissue-specific lipid remodeling and functional disruption in the colon and liver during early fatty liver disease

To define lipidomic alterations associated with early HFD-induced MASLD (HFD-16), we performed lipidomics on colon and liver tissues from MASLD and age-matched chow-fed controls (B6–16) (Fig. 5 and Supplementary Fig. 6). Broad shifts in individual lipid species were observed in both tissues, with the liver exhibiting a more extensive range of lipid changes than the colon, as shown in the volcano plots and fold-change plots (Fig. 5 A,B and Supplementary Fig. 6 A,B). Although numerous lipid features showed substantial fold-change differences, not all passed statistical significance thresholds ($p < 0.05$; $q < 0.1$ FDR).

In the colon, several lipid classes were consistently reduced, including sterols (ST), sulfonolipids (SL), cardiolipins (CL), and N-acyl glycyl serines (NaGlySer). ST and NaGlySer participate in microbial communication, energy balance, and cell-cell signaling, suggesting that MASLD disrupts host-microbe metabolic interactions at the level of the colon (Fig. 5 A,C). Depletion of SL, microbial-derived sphingolipid-like molecules involved in epithelial homeostasis, further points to impaired gut barrier integrity or perturbed microbial lipid signaling (Fig. 5 A,C). Reduced CL abundance, a mitochondrial membrane lipid essential for maintaining respiratory chain structure, is consistent with mitochondrial dysfunction and may contribute to a “leaky gut” phenotype through compromised colonocyte tight junction stability.

Lipid remodeling in the liver was more pronounced (Fig. 5B). MASLD livers accumulated members of the phosphatidylglycerol (PG), CL, and hemibismonoacylglycerophosphate (HBMP) classes, which support membrane curvature, vesicular trafficking, and intracellular signaling (Fig. 5 B,D). Elevated hepatic CL, a hallmark of mitochondrial stress, indicates early mitochondrial injury and cellular dysfunction in MASLD (Fig. 5 B,D). Similar to the colon, levels of SL, ST, and NaGlySer were decreased in the liver, along with reductions in sphingomyelins (SM) and diacylglycerols (DG), highlighting coordinated disruptions in sphingolipid-related and microbial-associated lipid pathways across tissues (Fig. 5B).

Class-level trends were further supported by lipid-specific heatmaps, which identified DG, phosphatidylcholines (PC), SL, and ST as consistently altered across both colon and liver (Fig. 5 C,D). Collectively, these findings suggest that early MASLD is accompanied by coupled intestinal and hepatic lipid remodeling, where impaired gut barrier function and colonocyte mitochondrial dysfunction may exacerbate hepatic stress and contribute to MASLD onset.

2.6. Tissue-specific lipid remodeling and functional disruption in the colon and liver during MASH

Lipidomic profiling of colon and liver tissues from MASH mice (HFD-29) revealed pronounced and tissue-specific shifts in lipid class composition relative to age-matched chow controls (B6–29) (Fig. 6 and Supplementary Fig. 7). In the colon (Fig. 6 A,C), several lipid classes including phosphatidylglycerols (PG), hexosylceramides (Hex2Cer), cardiolipins (CL), diacylglycerols (DG), and phosphatidylethanolamines (PE) were markedly elevated. Hex2Cer, a subclass of glycosphingolipids, is particularly notable because its accumulation suggests disrupted sphingolipid metabolism and potential impairment of lysosomal degradation pathways in the MASH colon. Increases in DG species, key intermediates in lipid signaling, may also contribute to tight-junction disruption and pro-inflammatory responses, consistent with known mechanisms linking DG accumulation to epithelial barrier dysfunction. In contrast, several members of the triglyceride (TG) class lipids involved in microbial communication, energy storage, and intercellular signaling were significantly decreased, indicating altered host-microbe metabolic interactions during MASH progression.

The liver displayed an even broader pattern of lipid remodeling (Fig. 6 B,D). MASH livers exhibited elevated levels of PG, PE, and hemibismonoacylglycerophosphates (HBMP), lipid classes implicated in membrane remodeling, vesicular trafficking, and cellular stress adaptation. These increases suggest compensatory restructuring of hepatocyte membranes in response to chronic injury. Conversely, multiple lipid classes including sterols (ST), sphingomyelins (SM), NaGlySer, lysophosphatidylethanolamines (LPE), TG, sulfonolipids (SL), and monogalactosyldiacylglycerols (SMGDG) were significantly reduced. Many of these lipids support membrane integrity, energy storage, and intracellular signaling, and their depletion reflects widespread disruption of hepatocellular homeostasis in advanced disease. Together, these findings demonstrate coordinated but tissue-specific lipidome reprogramming during MASH (Fig. 6 and Supplementary Fig. 7). The combined loss of signaling lipids, reductions in energy-storage TGs, and accumulation of stress-associated lipid species highlight profound remodeling of mitochondrial function, epithelial integrity, and gut-liver metabolic communication at this advanced stage of disease [38–40].

2.7. Alterations in circulating enteroendocrine cell hormones

Metabolomic analysis revealed increased levels of cholic acid across all tissue types in both MASLD and MASH samples (Table S3). Multiple studies have demonstrated that bile acids, including cholic acid, can activate EECs via takeda G protein-coupled receptor 5 (TGR5), a GPCR [41–45]. Supporting this, our pathway analysis indicated upregulation of signaling pathways associated with EEC function, including “Incretin synthesis, secretion, and inactivation”, “Synthesis, secretion, and

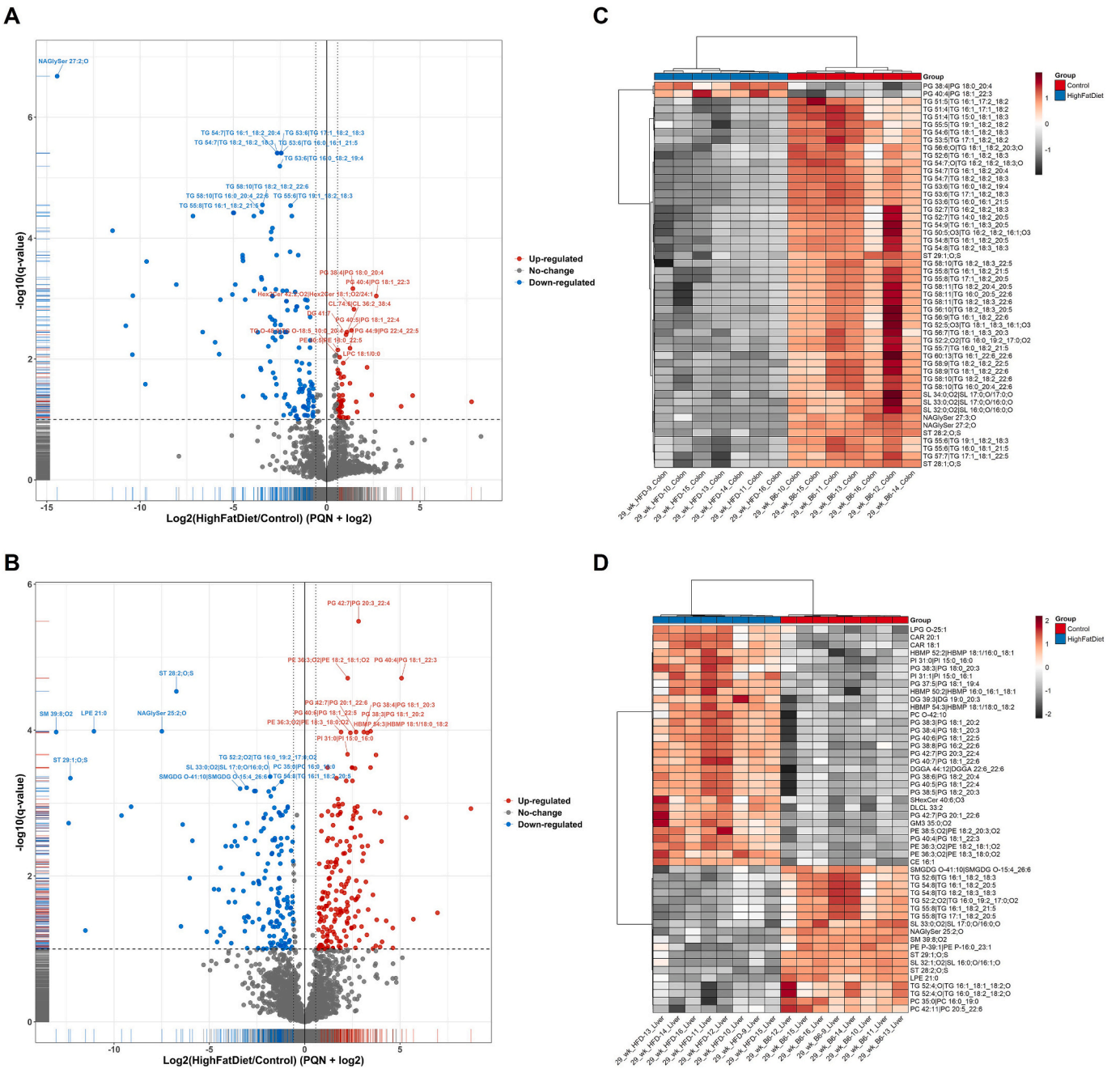

Fig. 6. Lipidomic alterations in the colon and liver of HFD-fed mice at 29 weeks Red dots show significantly upregulated and blue dots show significantly down-regulated lipid class members, grey dots show no change. (Nomenclature- Lipid member name Chain length: unsaturation). (A) The volcano plot shows the significantly altered individual members from specific lipid classes with chain length number and unsaturation in the colon of HFD-fed mice (HFD-29), with age-matched controls on normal chow diet as the reference based on log2-fold change and FDR $\leq$ 0.10 (positive and negative ionization modes combined). (**B**) The volcano plot shows the significantly altered individual members from specific lipid classes with chain length number and unsaturation in the liver of HFD-fed mice (HFD-29), with age-matched controls on normal chow diet as the reference based on log2-fold change and FDR $\leq$ 0.10 (positive and negative ionization modes combined). (**C**) This heat map shows top 50 quantitatively altered individual lipid members from specific classes with chain length number and unsaturation in the colon of HFD-fed mice (HFD-29), with age-matched controls on normal chow diet as the reference with sample and feature clustering. Features were ranked based on area. (**D**) This heat map shows top 50 quantitatively altered individual lipid members from specific classes with chain length number and unsaturation in the liver of HFD-fed mice (HFD-29), with age-matched controls on normal chow diet as the reference with sample and feature clustering. Features were ranked based on area. Table S4 details lipid abbreviation. (For interpretation of the references to color in this figure legend, the reader is referred to the web version of this article.)

inactivation of GLP-1" as well as "GPCR downstream signaling" and "GPCR ligand binding" in both colon and stool samples.

Based on these findings, we next examined circulating levels of enteroendocrine hormones, metabolic regulators as well as pro-inflammatory cytokines across our study groups. Plasma concentrations of GIP, GLP-1, peptide tyrosine tyrosine (PYY), ghrelin, secretin, 5-HT, insulin, amylin, pancreatic peptide (PP), C-peptide, leptin, and resistin were measured in HFD-16 and HFD-29 mice and compared to age-matched controls. Additionally, we quantified levels of the inflammatory cytokines tumor necrosis factor (TNF), interleukin-6 (IL-6), and *monocyte chemoattractant protein 1 (*MCP-1). In HFD-16 mice, we observed significant increases in GLP-1 (Fig. 7A), GIP (Fig. 7B), and PYY

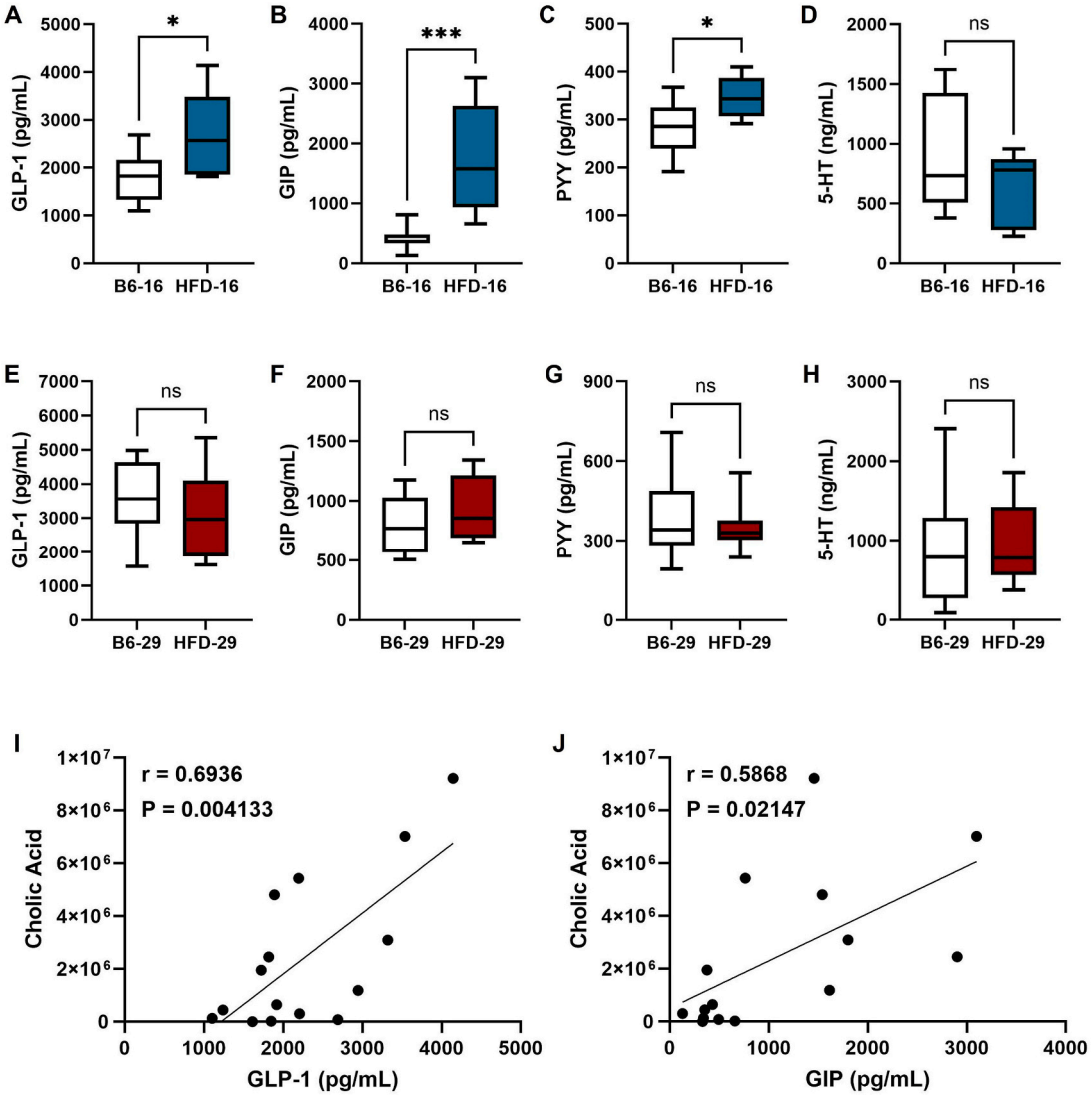

Fig. 7. Diet-induced changes in enteroendocrine hormones and their correlation with cholic acid levels. (**A-H**) Circulating levels of enteroendocrine hormones were measured in plasma from mice fed an HFD for 16 weeks (HFD-16) or 29 weeks (HFD-29) and compared to age-matched controls on a normal diet (B6–16 or B6–29). (**A-D**) B6–16 versus HFD-16 hormones (**A**) GLP-1, (**B**) GIP, (**C**) PYY, and (**D**) 5-HT. (***E*-H**) B6–29 versus HFD-29 hormones (**E**) GLP-1, (**F**) GIP, (**G**) PYY, and (**H**) 5-HT. (**I**, **J**) Colonic cholic acid levels positively correlated with (**I**) GLP-1 ($r = 0.6936$; $P = 0.004133$) and (**J**) GIP ($r = 0.5868$; $P = 0.02147$) levels in HFD-16 mice. *$P <$ 0.05, ***$P < 0.0005$, NS = not significant.

(Fig. 7C) compared to age-matched controls with no change in 5-HT (Fig. 8D), ghrelin (Supplementary Fig. 8A) or secretin (Supplementary Fig. 8C). In contrast, HFD-29 mice showed no significant difference in GLP-1 (Fig. 7E), GIP (Fig. 7F), PYY (Fig. 7G), 5-HT (Fig. 7H), ghrelin (Supplementary Fig. 8B) or secretin (Supplementary Fig. 8D) compared to age-matched controls. Notably, colonic cholic acid levels were positively correlated with GLP-1 ($r = 0.6936$; $p = 0.0041$) (Fig. 7I) and GIP levels ($r = 0.5868$; $p = 0.0214$) (Fig. 7J) in HFD-16 mice; however, no such correlation was observed in the HFD-29 group (data not shown).

We also found that HFD-16 mice had elevated plasma levels of insulin (Supplementary Fig. 8E), amylin (Supplementary Fig. 8G), leptin (Supplementary Fig. 8 M), resistin (Supplementary Fig. 8O), and TNF (Supplementary Fig. 8Q) compared to age-matched controls. Conversely, no differences in PP (Supplementary Fig. 8I), C-peptide (Supplementary Fig. 8 K), IL-6 (Supplementary Fig. 8S), or MCP-1 (Supplementary Fig. 8 U) were observed between groups. In HFD-29 mice, only TNF (Supplementary Fig. 8R) and IL-6 (Supplementary Fig. 8 T) were significantly increased compared to age-matched controls with no differences in insulin, amylin, PP, C-peptide, leptin, resistin or MCP-1 (Supplementary Fig. 8 F, H, J, L, N, P, and V). In summary, circulating levels of GLP-1, GIP, and PYY were significantly elevated in MASLD (HFD-16) mice and positively correlated with colonic cholic acid levels. These hormone levels were unchanged in MASH (HFD-29) mice, despite persistently elevated cholic acid, suggesting stage-specific alterations in EEC responsiveness. Furthermore, MASH mice exhibited increased TNF and IL-6 levels, indicative of a shift toward chronic inflammation with dampened incretin and metabolic hormone responses in later disease stages.

To determine whether these stage-specific differences in EEC abundance reflected intrinsic changes in epithelial differentiation potential, we next used organoid cultures derived from colonic crypts of each group. We collected colonic crypts from all groups to generate organoids, which were initially maintained in the intestinal stem cell state and then induced to differentiate by withdrawing WNT3A and R-spondin. Successful differentiation was confirmed by the expected reduction in *Lgr5* expression, a widely used stem cell marker (Supplementary Fig. 9 A, B, F, G). We next examined the expression of genes associated with the EEC lineage. For the 16-week groups, we observed no significant differences in *Neurog3*, *Chga*, or *Gcg* expression between organoids derived from B6–16 and HFD-16 mice (Supplementary Fig. 9C–E),

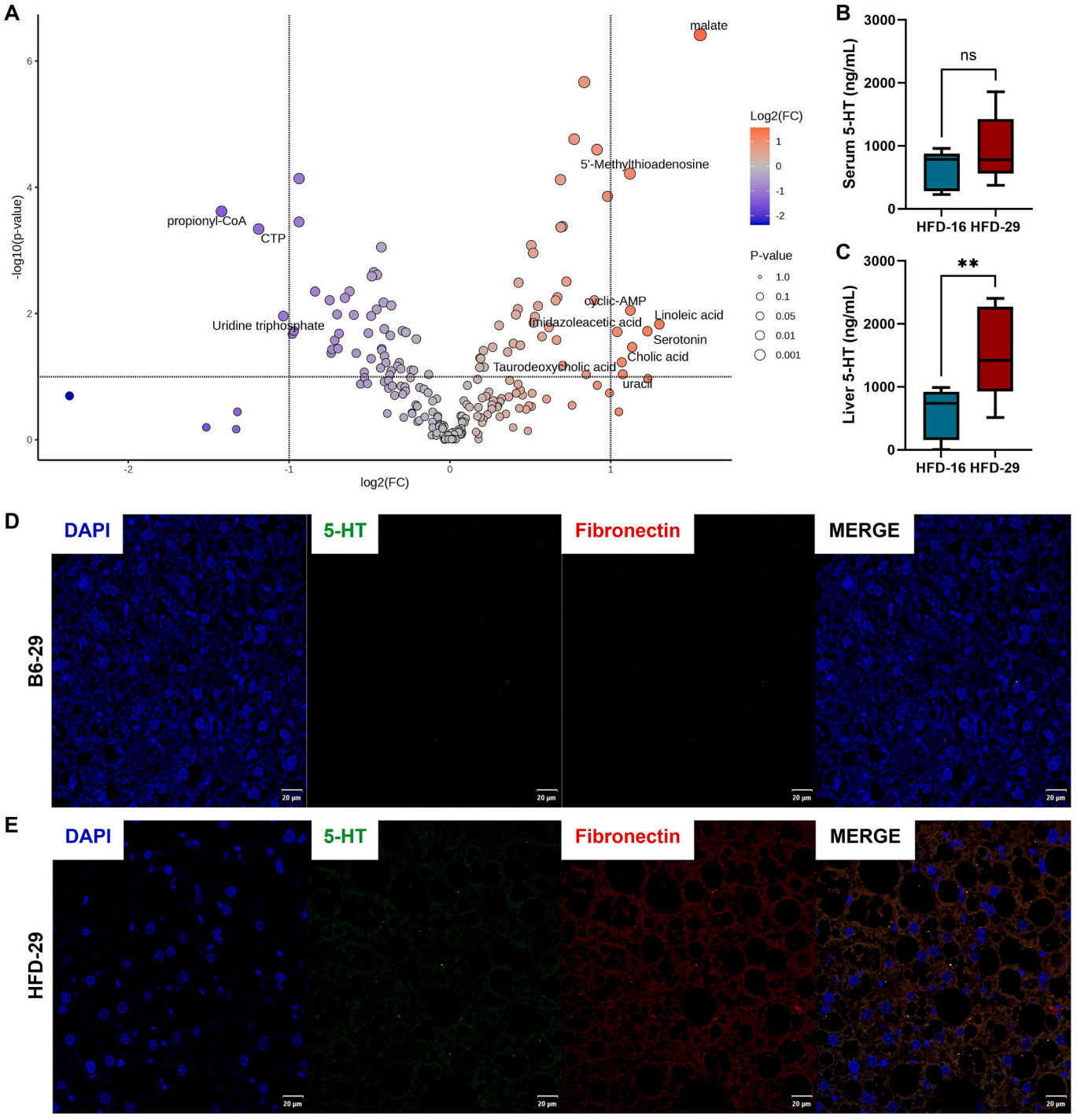

Fig. 8. Hepatic 5-HT and Fibronectin distribution in MASH mice. (**A**) Volcano plots show significantly altered hepatic metabolites in the HFD-29 compared to HFD-16 including 5-HT. Log_2 fold change (x-axis) is plotted against $-log_{10}$ (*p*-value) (y-axis), with dot size indicating significance level and color indicating directionality of change. (**B**, **C**) 5-HT levels as detected by ELISA were measured in (**B**) plasma and (**C**) liver tissues from HFD-16 (MASLD) and HFD-29 (MASH) mice. $n = 8$ mice per group. Data analyzed using Student's *t*-test. $^{**}P < 0.005$, NS = not significant. (**D**, **E**) Representative immunofluorescence images of DAPI, 5-HT, and fibronectin staining of liver sections in (**D**) control B6–29 and (**E**) HFD-29 livers.

indicating preserved EEC differentiation capacity at this stage. In contrast, at 29 weeks, organoids from HFD-fed mice showed a significant reduction in *Neurog3* and *Chga* expression compared to B6–29 controls, while *Gcg* expression remained unchanged (Supplementary Fig. 9H–J). These findings suggest that prolonged HFD exposure impairs EEC lineage specification and maturation, which may underlie the observed blunting of hormone responses in vivo during MASH progression.

To further evaluate EEC abundance in vivo, we performed immunofluorescence staining for chromogranin A (CHGA), a general marker of EECs, in colonic tissue. HFD-16 mice exhibited an increase in $CHGA^+$ cells within the colonic epithelium compared to age-matched controls, consistent with elevated circulating GLP-1 and PYY levels. In contrast, $CHGA^+$ cell abundance in HFD-29 mice was similar to that of their age-matched controls, aligning with the lack of hormone elevation at this later disease stage (Supplementary Fig. 10 A-D). Given the observed elevation in cholic acid and the established role of bile acid

signaling through TGR5 in regulating EEC function, we next examined colonic expression of TGR5 (Supplementary Fig. 10 E-L). Immunofluorescence analysis revealed a significant increase in mean TGR5 signal intensity in the colonic epithelium of HFD-16 mice compared to B6–16 controls, whereas no difference in TGR5 expression was detected between HFD-29 and B6–29 mice (Supplementary Fig. 10 M,N). These findings parallel the stage-specific elevation of circulating incretin hormones and their correlation with colonic cholic acid levels in HFD-16 mice, suggesting enhanced bile acid-TGR5 signaling during MASLD. In contrast, the absence of TGR5 upregulation in HFD-29 mice, despite persistently elevated cholic acid, is consistent with impaired epithelial responsiveness and blunted EEC signaling during MASH progression. Collectively, these data support a model in which early HFD exposure enhances bile acid-TGR5 signaling and EEC hormone output, whereas prolonged HFD feeding leads to intrinsic epithelial alterations that limit EEC differentiation and receptor responsiveness, contributing to the loss of incretin and metabolic hormone responses in advance diseases.

2.8. Metabolic and 5-HT alterations in the liver between MASLD and MASH

We compared metabolite differences between MASLD and MASH livers. MASH livers were found to have a significant increase in cholic acid, cyclic-AMP, imidazoleacetic acid, linoleic acid, malate, 5′-Methylthioadenosine, serotonin, taurodeoxycholic acid, and uracil (Fig. 8A). Interestingly, linoleic acid [46–48], 5′-Methylthioadenosine [49,50], and taurodeoxycholic acid [51,52] have all been linked to enhanced liver disease and inflammation. Given the known role of enterochromaffin cell-derived 5-HT in gut-liver signaling and fibrogenesis, we next compared 5-HT levels between HFD-16 (MASLD) and HFD-29 (MASH) mice. Plasma 5-HT levels were higher in HFD-29 mice compared to HFD-16 mice, although this trend did not reach statistical significance (Fig. 8B). When comparing 5-HT concentrations across compartments, hepatic levels in HFD-29 mice were significantly elevated compared to HFD-16 (Fig. 8C). Metabolomic profiling confirmed a significant increase in hepatic 5-HT levels in HFD-29 mice relative to HFD-16 mice (Fig. 8A), a difference that was not observed in the colon (data not shown), suggesting local 5-HT accumulation or impaired hepatic clearance in the context of MASH.

To examine whether this increase in hepatic 5-HT was associated with fibrotic remodeling, we performed immunofluorescence staining for fibronectin, a key extracellular matrix protein and marker of liver fibrosis. HFD-29 livers displayed marked fibronectin deposition (Fig. 8E), which was not detected in B6–29 controls (Fig. 8D). Importantly, 5-HT staining in HFD-29 livers showed partial co-localization with fibronectin-positive regions, suggesting that 5-HT accumulates within or contributes to fibrotic microenvironments (Fig. 8E). Although Pearson's correlation analysis (data not shown) did not reveal a significant spatial correlation between 5-HT and fibronectin staining, the increased hepatic abundance of 5-HT in HFD-29 mice suggests altered hepatic handling of 5-HT in the context of fibrotic remodeling. These findings raise the possibility that chronic HFD exposure leads to a shift in EEC-derived 5-HT distribution, promoting its hepatic retention and potential involvement in fibrosis during the transition from MASLD to MASH.

3. Discussion

In this study, we leveraged a well-established dietary model to investigate how chronic HFD [30,31] exposure drives progression from MASLD and MASH, with a specific focus on the gut-liver axis. Using integrated metabolomic, lipidomic, hormonal, and histological approaches, we demonstrate that this transition is marked by dynamic, stage-specific changes in EEC activity, metabolic hormone output, and 5-HT distribution. During early disease (MASLD), HFD-fed mice exhibited elevated levels of GLP-1, GIP, and PYY in the circulation, which correlated with increased cholic acid in the colon and liver and increased $TGR5^{+}CHGA^{+}$ cell abundance in the colonic epithelium. Conversely, with prolonged HFD feeding and progression to MASH, these hormone elevations were lost despite persistent cholic acid elevation, suggesting a blunting or silencing of EEC responsiveness. This was supported by reduced expression of EEC lineage markers (*Neurog3*, *Chga*) in colonic organoids derived from HFD-29 mice as well as the absence of TGR5 upregulation in the colonic epithelium at the MASH stage. Concomitantly, hepatic 5-HT levels were significantly increased in MASH, with partial co-localization to fibronectin-rich regions, implicating 5-HT in fibrotic remodeling. To assess this relationship, we performed quantitative colocalization analysis of 5-HT and fibronectin signals. Although 5-HT was frequently observed in proximity to fibrotic areas, Pearson's correlation coefficients were not significantly different between groups, indicating that this association is spatially suggestive rather than functionally definitive. This observation aligns with previous studies showing 5-HT promotes hepatic stellate cell activation via the 5-HT2B receptor, stimulating TGF-β and collagen production [53–55]. However, as no genetic or pharmacologic manipulation of 5-HT or EEC pathways were performed in this study, these findings should be interpreted as correlative and hypothesis-generating. Together, these data identify a temporal reprogramming of gut endocrine signaling across MASLD-to-MASH progression and highlight potential mechanistic links between EEC dysfunction, bile acid signaling, and hepatic fibrosis.

The observed changes in hormone output have important implications for systemic metabolic regulation. GIP and GLP-1 act as incretins that enhance insulin secretion following nutrient intake [56], while PYY contributes to appetite suppression and reduced gastrointestinal motility [57]. Insulin and amylin maintain glucose homeostasis [58]; leptin regulates energy balance and satiety [59]; and resistin has been linked to inflammation and insulin resistance [60,61]. Our observation that MASLD mice exhibit elevated fed-state GLP-1, GIP, and PYY levels contrasts with clinical studies reporting an insufficient stimulated GLP-1 response in patients with MASLD [62]. Several factors may explain this divergence. In rodent models, chronic high-fat feeding can induce an early compensatory increase in EEC hormone secretion, driven in part by enhanced bile acid-mediated L cell stimulation (including elevated cholic acid), altered nutrient transit, and intestinal remodeling [63–65]. In humans, however, metabolic disease is frequently associated with impaired nutrient-triggered incretin release, even when fasting or fed-state levels appear normal [62]. This relative failure of stimulated GLP-1 secretion likely contributes to metabolic dysfunction and may help explain the strong therapeutic efficacy of GLP-1 receptor agonists and dual GIP/GLP-1 agonist such as liraglutide, semaglutide, and tirzepatide, which overcome this physiological deficit. Thus, while our findings highlight potential bile acid-driven enhancement of incretin secretion in early disease of mice it also suggests that progressive metabolic dysfunction, as seen in humans, may ultimately blunt nutrient-stimulated EEC responses. This distinction underscores the importance of evaluating both basal and stimulated GLP-1 secretion across species and disease stages. Observations in zebrafish show microbiota-dependent EEC silencing and highlight the dynamic plasticity of the gut endocrine system in response to chronic nutritional stress [66]. Several studies support the broader concept that EEC lineage commitment is strongly regulated at the epigenetic level, making NEUROG3, an EEC-commitment factor, a target of metabolic or inflammatory stress. NEUROG3 expression depends on chromatin remodeling events including removal of repressive H3K27me3 marks during the transition from low to high NEUROG3 EEC progenitors [67]. NEUROG3 dosage itself is a key determinant of ECC versus goblet cell fate [68] and complete loss of NEUROG3 functions in humans and mice results in a total absence of EEC [69,70]. Additionally, metabolic stressors such as a HFD are known to induce DNA methylation-dependent silencing of EEC regulatory genes in other tissues [71], providing a mechanistic precedent for similar epigenetic repression of

NEUROG3 in the intestine. Our data reveal a time-dependent adaptation of enteroendocrine signaling to an HFD. At 16 weeks, HFD-fed mice exhibit elevated circulating levels of GLP-1, GIP, and PYY, consistent with EEC hyperactivation. Supporting this, organoids derived from HFD-16 and control mice showed no significant differences in the expression of EEC lineage genes (*Neurog3*, *Chga*, *Gcg*), suggesting intact differentiation capacity. However, by 29 weeks, hormone levels are comparable to age-matched controls, indicative of EEC desensitization or functional remodeling. In support of this, HFD-29-derived organoids show significant reductions in *Neurog3* and *Chga* expression, pointing to impaired EEC lineage commitment and maturation. Interestingly, 5-HT levels increase significantly in the liver at this stage, implicating a potential shift in EEC subtype activity, favoring enterochromaffin cell output or microbiota-mediated stimulation of 5-HT biosynthesis. Notably, several pathways altered in our murine dataset align with hormonal signatures reported in human MASLD and MASH. Human studies have documented increased circulating 5-HT in patients with MASLD and MASH [26] suggesting a role for peripheral 5-HT in disease severity. Additionally, EEC hormones such as GLP-1 and GIP are implicated in systemic metabolic regulation in humans and are therapeutic targets in MASLD and MASH clinical trials [21,72]. To this end, dedicated validation in human MASLD and MASH cohorts including direct assessment of EEC markers, serotonergic regulators, and circulating or tissue 5-HT levels will be essential to confirm and extend the mechanistic hypothesis generated by this study.

The results from the metabolomics analysis of liver, colon, and stool tissues highlight significant metabolic disturbances in mice on an HFD, with increasing severity from MASLD to MASH. The key trend of cholic acid accumulation across all tissues suggests an impairment in bile acid metabolism, potentially pointing to disrupted enterohepatic circulation and altered bile acid synthesis. Importantly, several pathways altered in our murine dataset, including EEC remodeling and bile acid-linked GLP-1 signaling align with associations previously reported in human and animal studies. Bile acids, which are synthesized in the liver and released into the small intestine, are crucial regulators of metabolic processes such as lipid metabolism, glucose homeostasis, and liver injury. Activation of the bile acid receptor TGR5 has been shown to induce intestinal GLP-1 release and improve glucose homeostasis [64,65]. Dysregulation of bile acid metabolism, both in the liver and the gut, has been implicated in the pathogenesis of MASLD and MASH [73,74]. Altered bile acid profiles, including increased levels of cholic acid, have been associated with hepatic steatosis, inflammation, and fibrosis in both animal models [75–77] and human patients [78]. Furthermore, bile acids modulate the gut microbiota, influencing liver inflammation and fibrosis, suggesting a complex interaction between bile acid signaling and the gut-liver axis in disease progression. We hypothesize that bile acids may interact with EECs in the gut, stimulating the release of hormones such as GLP-1, PYY, and GIP that support lipid metabolism and hepatic function during early disease. Over time, however, persistent cholic acid elevation may contribute to EEC dysfunction or desensitization, disrupting gut hormone signaling and weakening the protective gut-liver feedback loop. This could facilitate progression from steatosis to steatohepatitis and systemic metabolic derangement. Additionally, both HFD groups showed downregulation of various amino acid metabolites and energy-related metabolites, with further dysregulation observed in the MASH group, indicating a progression toward more severe liver disease. The data also suggest that prolonged HFD exposure leads to gut microbiota changes, as evidenced by altered stool metabolite profiles.

Although we did not perform microbiota sequencing in this study, our metabolomics data show microbial contributions, particularly in pathways such as tryptophan-kynurenine metabolism and bile acid-microbiome interactions. These microbial linked signatures are consistent with several human studies showing gut dysbiosis in MASLD and MASH patients. For example, it was reported that increasing disease severity is associated with shifts in microbial taxa and enrichment of microbial pathways related to carbohydrate, lipid, and amino acid metabolism, including aromatic amino acid turnover [79]. Similarly, another study demonstrated that gut microbiome composition and microbial metabolic functions can stratify fibrosis severity in MASLD [80], while another study showed that MASLD is accompanied by reduced microbial diversity and strong correlations between microbiome composition and circulating metabolites [81]. Another metabolite, short chain fatty acids (SCFA), microbial fermentation products of dietary fiber, directly stimulate colonic L cells to secrete GLP-1 and PYY [82]. Altered SCFA production due to dysbiosis, as suggested by our metabolomics data, could contribute to impaired EEC signaling and blunted incretin responses during MASLD to MASH progression. Together, these human data support the relevance of the microbial metabolic disturbances detected in our murine model, while underscoring the need for future studies incorporating parallel microbiome profiling. Overall, these findings provide novel insights into the metabolic shifts occurring in the liver, colon, and stool, and underscore the complex relationship between diet, metabolic dysregulation, and the progression of simple steatosis to steatohepatitis.

Further investigation into the specific roles of these metabolites in disease progression could provide valuable targets for therapeutic intervention. While GLP-1 receptor agonists and dual GIP/GLP-1 agonist like tirzepatide have shown promise in improving metabolic parameters and reducing hepatic steatosis in preclinical and early clinical studies, their long-term efficacy in treating MASLD and MASH remains under active investigation. Clinical experience with these agents, particularly in liver disease, is still evolving, and questions remain regarding the magnitude and durability of their therapeutic effects on hepatic inflammation and fibrosis. To further contextualize these metabolomics changes within a human disease framework, we integrated mouse-derived metabolites with human-annotated pathway and chemical ontology databases (RaMP-DB). These pathway enrichment analyses were intended as hypothesis-generating and interpretive tools, rather than as evidenced of conserved or causal mechanisms across species. Given know interspecies differences in metabolic pathway organization and regulation, enrichment concordance should be viewed as suggestive rather than definitive. Because metabolites were profiled across multiple compartments, including liver, colon, and stool, pathway mapping reflects biologically related but compartment-specific processes. Accordingly, these associations should be interpreted as reflective of coordinated gut-liver metabolic remodeling rather than direct compartment-to-compartment equivalence.

Lipidomic analysis of the liver and colon revealed dynamic, tissue-specific remodeling of lipid classes that parallels the progression from MASLD to MASH in HFD-fed mice. In the MASLD stage, the liver displayed a robust upregulation of free fatty acids (FAs), an early and well-documented hallmark of hepatic steatosis and lipid overload in MASLD pathogenesis [39,83]. As key precursors for complex lipid biosynthesis, the elevation of FAs is consistent with the metabolic shift toward hepatic lipid accumulation. Accompanying this, both the liver and colon showed increased levels of diacylglycerols (DG), a lipid class directly linked to hepatic insulin resistance and metabolic dysfunction [84], thereby reinforcing the connection between lipid dysregulation and disease progression. Additionally, MASLD tissues exhibited higher levels of lysophosphatidylcholine (LPC) and lysophosphatidylethanolamine (LPE), bioactive lipid classes known to induce lipotoxicity in hepatocytes and contribute to inflammatory signaling cascades [85]. Together, the upregulation of FAs, DG, LPC, and LPE in MASLD suggests a coordinated lipotoxic program that promotes metabolic stress and may predispose tissues to further injury and progression toward MASH.

In contrast, the MASH phenotype was marked by a distinct shift in lipid signatures. Notably, acylcarnitines (CAR) were the only lipid class consistently increased in both liver and colon of MASH mice. As intermediates of mitochondrial fatty acid oxidation, elevated CAR levels indicate mitochondrial overload or incomplete β-oxidation, which is a hallmark of advanced liver pathology. Furthermore, CAR accumulation

has been associated with hepatocellular carcinoma (HCC), suggesting that their elevation in MASH may reflect a metabolic trajectory toward oncogenic transformation [86]. Thus, CAR species may serve as early biomarkers for MASH severity and its potential progression to liver cancer.

Additional patterns of lipid remodeling further distinguish MASLD from MASH. Phosphatidylethanolamines (PE), essential components of membrane structure and lipid bilayer integrity, were elevated in MASLD liver but significantly reduced in MASH liver, mirroring previous observations that PE depletion correlates with disease advancement [87]. A consistent downregulation of sulfonolipids (SL) in both liver and colon across disease stages provides further mechanistic insight into gut-liver communication. As microbiota-derived lipids structurally analogous to sphingolipids, SLs are emerging mediators of immune homeostasis and epithelial integrity [88]. Their depletion supports the hypothesis that microbial lipid signaling is disrupted in the context of MASLD/MASH, contributing to immune dysregulation and disease progression.

These lipid alterations may also influence bile acid composition and enteroendocrine cell function, potentially linking shifts in membrane remodeling and mitochondrial metabolism to changes in gut-liver hormonal and metabolic signaling. Together, these findings highlight that MASLD and MASH are characterized by distinct lipidomic signatures reflecting early lipotoxic stress (FAs, DG, LPC/LPE), mitochondrial dysfunction (CAR), and disrupted host-microbial signaling (SL). These tissue-specific lipid alterations offer mechanistic insight into the gut-liver axis in metabolic liver disease and may serve as candidate biomarkers for disease stage and therapeutic targeting.

3.1. Limitation of study

This study has several limitations. First, while we observed dynamic changes in circulating and tissue hormone levels, we did not directly assess the functional metabolic consequences of altered enteroendocrine signaling, such as insulin secretion, appetite regulation, or hepatic glucose handling. GLP-1 was measured in the fed state, reflecting physiological secretion during nutrient intake; however, stimulated incretin responses following standardized nutrient challenges were not assessed and warrant future investigation.

Second, although our data suggest EEC desensitization and impaired lineage commitment with prolonged HFD exposure, we did not employ genetic or pharmacologic approaches to causally manipulate EEC differentiation, bile acid signaling, or serotonergic pathways. Microbiota composition was not directly profiled, and microbial contribution to EEC remodeling were inferred from metabolomics signatures and prior literature [66,89–91]. Additionally, organoid analyses were performed at the bulk level, limiting resolution of specific EEC subtypes. Future studies using single-cell approaches will be important to define subtype-specific remodeling.

Third, 5-HT localization in fibronectin-rich regions suggests a spatial association with hepatic fibrosis, but higher-resolution imaging and mechanistic studies are needed to define cellular sources and functional roles. Finally, this work conducted exclusively in a male murine dietary model of MASLD and MASH, which captures only a subset of features of human disease. Species-specific differences in metabolism, immune responses, gut hormone regulation, and fibrosis progression constrain direct translation. While the use of male mice reduced variability, sex-specific differences in MASLD susceptibility and gut-liver signaling are well documented and should be addressed in future studies.

3.2. Strengths, translational relevance, and future directions

Despite these limitations, this study provides several important strengths, including longitudinal characterization of gut-liver enteroendocrine remodeling across progressive stages of diet-induced MASLD and MASH using integrated histologic, transcriptomic, metabolomic, and organoid-based approaches. The identification of coordinated alterations in GLP-1, bile acid signaling, serotonergic pathways, and enteroendocrine lineage programs highlights potentially targetable mechanisms linking intestinal dysfunction with hepatic disease progression. These findings have translational relevance, as incretin-based therapies and modulators of bile acid and gut-derived signaling pathways are increasingly being explored in MASLD/MASH treatment. Our results suggest that progressive impairment of enteroendocrine adaptation may contribute to disease progression and therapeutic responsiveness, supporting further investigation of gut-liver endocrine signaling as both a biomarker axis and therapeutic target in human MASLD and MASH.

4. Materials and methods

Detailed ‘Materials and methods’ are provided in the supplementary information.

Abbreviations

2-PY	*N*-methyl-2-pyridone-5-carboxamide
5-HT	Serotonin
CHGA	chromogranin A
EEC	Enteroendocrine cells
HFD	High-Fat Diet
IL-6	Interleukin-6
GIP	Glucose-dependent Insulinotropic Polypeptide
GLP-1	Glucagon-like Peptide-1
GPCR	G Protein-Coupled Receptor
LCN-2	Lipocalin-2
LGR5	Leucine-rich repeat-containing G-protein coupled receptor 5
MASLD	Metabolic Dysfunction-Associated Steatotic Liver Disease
MASH	Metabolic Dysfunction-Associated Steatohepatitis
MCP-1	*Monocyte Chemoattractant Protein 1*
NAD	Nicotinamide Adenine Dinucleotide
PP	Pancreatic Peptide
PYY	Peptide tyrosine tyrosine
RaMP-DB	Relational database of Metabolomic Pathways
TGR5	Takeda G protein-coupled Receptor 5
TNF	Tumor Necrosis Factor

CRediT authorship contribution statement

Jaclyn A. Rivas: Writing – review & editing, Writing – original draft, Visualization, Validation, Software, Resources, Methodology, Investigation, Formal analysis, Data curation, Conceptualization. **Alexandria C. Murphy:** Writing – review & editing, Writing – original draft, Visualization, Validation, Resources, Methodology, Investigation, Data curation, Conceptualization. **Praveena Prasad:** Writing – review & editing, Visualization, Software, Investigation, Formal analysis, Data curation. **Mahmoud S. Yahia:** Methodology, Formal analysis. **Siem S. Goitom:** Writing – review & editing, Investigation. **Aaron S. Romero:** Writing – review & editing, Investigation. **Crystal Madera Enriquez:** Writing – review & editing, Investigation. **Brianna B. Maes:** Writing – review & editing, Investigation. **Prithvi R. Akepati:** Writing – review & editing, Investigation. **Marcus A. Garcia:** Writing – review & editing, Investigation. **Fredine T. Lauer:** Writing – review & editing, Resources, Methodology, Investigation. **Rama R. Gullapalli:** Writing – review & editing, Resources, Investigation, Formal analysis. **Kristen M. Gonzales:** Writing – review & editing, Writing – original draft, Formal analysis. **Jessica M. Gross:** Writing – review & editing, Formal analysis. **Jing Pu:** Writing – review & editing, Investigation, Formal analysis. **Shuguang Leng:** Writing – review & editing, Resources. **Julie G. In:** Writing – review & editing, Resources. **Melanie R. McReynolds:** Writing – review & editing, Writing – original draft, Visualization, Validation, Supervision, Resources, Project administration, Methodology, Investigation, Funding acquisition, Formal analysis, Data curation,

Conceptualization. **Eliseo F. Castillo:** Writing – review & editing, Writing – original draft, Visualization, Validation, Supervision, Resources, Project administration, Methodology, Investigation, Funding acquisition, Formal analysis, Data curation, Conceptualization.

Financial support

This work was supported by Institutional Research Grant IRG-21-146-25 from the American Cancer Society (E.F.C.); the UNM Comprehensive Cancer Center Support Grant NCI P30CA118100 (E.F.C.) and the Human Tissue Repository, Tissue Analysis, and Fluorescence Microscopy Shared Resources cores; the National Center for Research Resources and the National Center for Advancing Translational Sciences of the National Institutes of Health through grants UL1TR001449 (E.F.C.) and P20GM121176 (E.F.C.); and the training grant T32 GM144834, which supported J.A.R. and B.B.M. Additional support was provided by the Howard Hughes Medical Institute Hanna H. Gray Fellows Program Faculty Phase (Grant #GT15655, awarded to M.R.M.) and the Burroughs Wellcome Fund PDEP Transition to Faculty (Grant #1022604, awarded to M.R.M.).

Declaration of competing interest

The authors have declared that no personal or financial competing interests exist.

Acknowledgments

We would also like to acknowledge the Huck Institutes' Metabolomics Core Facility (RRID: SCR_023864) for use of the OE 240 LCMS and Sergei Koshkin for helpful discussions on sample preparation and analysis. During the preparation of this work the author(s) used ChatGPT in order to improve the clarity and readability of the *Results* section. After using this tool, the author(s) reviewed and edited the content as needed and take(s) full responsibility for the content of the publication. We further acknowledge the UNM Comprehensive Cancer Center Support Grant NCI P30CA118100 and the HSC Shared Equipment for use of the Olympus iX83 Yokogawa Spinning Disk Confocal Microscope and Evident APEXVIEW APX100 Benchtop Fluorescence Microscope within the Advanced Light Microscopy Resource. We thank Michael L. Paffett at the UNM Advanced Light Microscopy Resource for training and guidance with confocal imaging. Graphical Abstract was created with BioRender.com.

Appendix A. Supplementary data

Supplementary data to this article can be found online at https://doi.org/10.1016/j.metabol.2026.156652.

Data availability

All primary data associated with this study are present in the paper or the Supplementary Materials.

References

[1] Feng G, Targher G, Byrne CD, Yilmaz Y, Wai-Sun Wong V, Adithya Lesmana CR, et al. Global burden of metabolic dysfunction-associated steatotic liver disease, 2010 to 2021. JHEP Rep. 2025;7:101271.
[2] Younossi ZM, Kalligeros M, Henry L. Epidemiology of metabolic dysfunction-associated steatotic liver disease. Clin Mol Hepatol. 2025;31:S32–50.
[3] Le P, Tatar M, Dasarathy S, Alkhouri N, Herman WH, Taksler GB, et al. Estimated burden of metabolic dysfunction-associated steatotic liver disease in US adults, 2020 to 2050. JAMA Netw Open. 2025;8:e2454707.
[4] Byrne CD, Armandi A, Pellegrinelli V, Vidal-Puig A, Bugianesi E. Metabolic dysfunction-associated steatotic liver disease: a condition of heterogeneous metabolic risk factors, mechanisms and comorbidities requiring holistic treatment. Nat Rev Gastroenterol Hepatol 2025;22(5):314–28.
[5] Kalligeros M, Henry L, Younossi ZM. Metabolic dysfunction-associated steatotic liver disease and its link to cancer. Metabolism 2024;160:156004.
[6] Mantovani A, Lonardo A, Stefan N, Targher G. Metabolic dysfunction-associated steatotic liver disease and extrahepatic gastrointestinal cancers. Metabolism 2024;160:156014.
[7] Armandi A, Rosso C, Caviglia GP, Bugianesi E. An updated overview on hepatocellular carcinoma in patients with metabolic dysfunction-associated steatotic liver disease: trends, pathophysiology and risk-based surveillance. Metabolism 2025;162:156080.
[8] Larraufie P, Roberts GP, McGavigan AK, Kay RG, Li J, Leiter A, et al. Important role of the GLP-1 axis for glucose homeostasis after bariatric surgery. Cell Rep. 2019;26(1399–408):e6.
[9] Baggio LL, Drucker DJ. Biology of incretins: GLP-1 and GIP. Gastroenterology 2007;132:2131–57.
[10] Yen FS, Hou MC, Cheng-Chung Wei J, Shih YH, Hsu CY, Hsu CC, et al. Glucagon-like peptide-1 receptor agonist use in patients with liver cirrhosis and type 2 diabetes. Clin Gastroenterol Hepatol. 2024;22(1255–64):e18.
[11] Havranek B, Loh R, Torre B, Redfield R, Halegoua-DeMarzio D. Glucagon-like peptide-1 receptor agonists improve metabolic dysfunction-associated steatotic liver disease outcomes. Sci Rep. 2025;15:4947.
[12] Armstrong MJ, Houlihan DD, Rowe IA, Clausen WH, Elbrond B, Gough SC, et al. Safety and efficacy of liraglutide in patients with type 2 diabetes and elevated liver enzymes: individual patient data meta-analysis of the LEAD program. Aliment Pharmacol Ther. 2013;37:234–42.
[13] Armstrong MJ, Gaunt P, Aithal GP, Barton D, Hull D, Parker R, et al. Liraglutide safety and efficacy in patients with non-alcoholic steatohepatitis (LEAN): a multicentre, double-blind, randomised, placebo-controlled phase 2 study. Lancet 2016;387:679–90.
[14] Kelly AS, Auerbach P, Barrientos-Perez M, Gies I, Hale PM, Marcus C, et al. A randomized, controlled trial of liraglutide for adolescents with obesity. N Engl J Med. 2020;382:2117–28.
[15] Newsome PN, Buchholtz K, Cusi K, Linder M, Okanoue T, Ratziu V, et al. A placebo-controlled trial of subcutaneous semaglutide in nonalcoholic steatohepatitis. N Engl J Med. 2021;384:1113–24.
[16] Jensen EL, Israelsen M, Krag A. Transforming steatotic liver disease management: the emerging role of GLP-1 receptor agonists. Hepatol Commun. 2024:8.
[17] Stefanakis K, Gutierrez de Pineres V, Veeragandham P, Mantzoros CS. Proteomic effects of short-term liraglutide vs. placebo in a blinded crossover RCT: Implications for efficacy, safety, and comparison with semaglutide. Metabolism 2026;177:156493.
[18] Zhang J, Guan X, Kong M, Xia M, Yu Y, Zhang C. GLP-1RAs and tirzepatide may reduce heart failure risk in obese but not in non-obese patients with cardiovascular or renal disease: a systematic review and meta-analysis. Metabolism 2026;175:156433.
[19] Karakasis P, Patoulias D, Fragakis N, Mantzoros CS. Effect of glucagon-like peptide-1 receptor agonists and co-agonists on body composition: systematic review and network meta-analysis. Metabolism 2025;164:156113.
[20] Heise T, Mari A, DeVries JH, Urva S, Li J, Pratt EJ, et al. Effects of subcutaneous tirzepatide versus placebo or semaglutide on pancreatic islet function and insulin sensitivity in adults with type 2 diabetes: a multicentre, randomised, double-blind, parallel-arm, phase 1 clinical trial. Lancet Diabetes Endocrinol. 2022;10:418–29.
[21] Loomba R, Hartman ML, Lawitz EJ, Vuppalanchi R, Boursier J, Bugianesi E, et al. Tirzepatide for metabolic dysfunction-associated steatohepatitis with liver fibrosis. N Engl J Med. 2024;391:299–310.
[22] Barter R, Pearse AG. Detection of 5-hydroxytryptamine in mammalian enterochromaffin cells. Nature 1953;172:810.
[23] Erspamer V, Asero B. Identification of enteramine, the specific hormone of the enterochromaffin cell system, as 5-hydroxytryptamine. Nature 1952;169:800–1.
[24] Mao B, Liu S, Zhu S, Wu F, Yuan W, Yan Y, et al. The janus face of serotonin: regenerative promoter and chronic liver disease aggravator. Heliyon 2024;10:e30703.
[25] Choi W, Namkung J, Hwang I, Kim H, Lim A, Park HJ, et al. Serotonin signals through a gut-liver axis to regulate hepatic steatosis. Nat Commun. 2018;9:4824.
[26] Wang L, Fan X, Han J, Cai M, Wang X, Wang Y, et al. Gut-derived serotonin contributes to the progression of non-alcoholic steatohepatitis via the liver HTR2A/PPARgamma2 pathway. Front Pharmacol. 2020;11:553.
[27] Martin AM, Young RL, Leong L, Rogers GB, Spencer NJ, Jessup CF, et al. The diverse metabolic roles of peripheral serotonin. Endocrinology 2017;158:1049–63.
[28] Watanabe H, Rose MT, Aso H. Role of peripheral serotonin in glucose and lipid metabolism. Curr Opin Lipidol. 2011;22:186–91.
[29] Liu N, Sun S, Wang P, Sun Y, Hu Q, Wang X. The mechanism of secretion and metabolism of gut-derived 5-hydroxytryptamine. Int J Mol Sci. 2021;22.
[30] Kristiansen MN, Veidal SS, Rigbolt KT, Tolbol KS, Roth JD, Jelsing J, et al. Obese diet-induced mouse models of nonalcoholic steatohepatitis-tracking disease by liver biopsy. World J Hepatol. 2016;8:673–84.
[31] Trevaskis JL, Griffin PS, Wittmer C, Neuschwander-Tetri BA, Brunt EM, Dolman CS, et al. Glucagon-like peptide-1 receptor agonism improves metabolic, biochemical, and histopathological indices of nonalcoholic steatohepatitis in mice. Am J Physiol Gastrointest Liver Physiol. 2012;302:G762–72.
[32] Raffatellu M, George MD, Akiyama Y, Hornsby MJ, Nuccio SP, Paixao TA, et al. Lipocalin-2 resistance confers an advantage to Salmonella enterica serotype Typhimurium for growth and survival in the inflamed intestine. Cell Host Microbe. 2009;5:476–86.
[33] Playford RJ, Belo A, Poulsom R, Fitzgerald AJ, Harris K, Pawluczyk I, et al. Effects of mouse and human lipocalin homologues 24p3/lcn2 and neutrophil gelatinase-

associated lipocalin on gastrointestinal mucosal integrity and repair. Gastroenterology 2006;131:809–17.
[34] Chassaing B, Srinivasan G, Delgado MA, Young AN, Gewirtz AT, Vijay-Kumar M. Fecal lipocalin 2, a sensitive and broadly dynamic non-invasive biomarker for intestinal inflammation. PLoS One. 2012;7:e44328.
[35] Braisted J, Patt A, Tindall C, Sheils T, Neyra J, Spencer K, et al. RaMP-DB 2.0: a renovated knowledgebase for deriving biological and chemical insight from metabolites, proteins, and genes. Bioinformatics 2023:39.
[36] Shannon P, Markiel A, Ozier O, Baliga NS, Wang JT, Ramage D, et al. Cytoscape: a software environment for integrated models of biomolecular interaction networks. Genome Res. 2003;13:2498–504.
[37] Goenawan IH, Bryan K, Lynn DJ. DyNet: visualization and analysis of dynamic molecular interaction networks. Bioinformatics 2016;32:2713–5.
[38] Gruevska A, Leslie J, Perpinan E, Maude H, Collins AL, Johnson S, et al. Spatial lipidomics reveals sphingolipid metabolism as anti-fibrotic target in the liver. Metabolism 2025;168:156237.
[39] Muralidharan S, Lee JWJ, Lim YS, Muthiah M, Tan E, Demicioglu D, et al. Serum lipidomic signatures in patients with varying histological severity of metabolic-dysfunction associated steatotic liver disease. Metabolism 2025;162:156063.
[40] Vouilloz A, Bourgeois T, Diedisheim M, Pilot T, Jalil A, Le Guern N, et al. Impaired unsaturated fatty acid elongation alters mitochondrial function and accelerates metabolic dysfunction-associated steatohepatitis progression. Metabolism 2025;162:156051.
[41] Hansen M, Scheltema MJ, Sonne DP, Hansen JS, Sperling M, Rehfeld JF, et al. Effect of chenodeoxycholic acid and the bile acid sequestrant colesevelam on glucagon-like peptide-1 secretion. Diabetes Obes Metab. 2016;18:571–80.
[42] Katsuma S, Hirasawa A, Tsujimoto G. Bile acids promote glucagon-like peptide-1 secretion through TGR5 in a murine enteroendocrine cell line STC-1. Biochem Biophys Res Commun. 2005;329:386–90.
[43] Calderon G, McRae A, Rievaj J, Davis J, Zandvakili I, Linker-Nord S, et al. Ileo-colonic delivery of conjugated bile acids improves glucose homeostasis via colonic GLP-1-producing enteroendocrine cells in human obesity and diabetes. EBioMedicine 2020;55:102759.
[44] Parker HE, Wallis K, le Roux CW, Wong KY, Reimann F, Gribble FM. Molecular mechanisms underlying bile acid-stimulated glucagon-like peptide-1 secretion. Br J Pharmacol. 2012;165:414–23.
[45] Christiansen CB, Trammell SAJ, Wewer Albrechtsen NJ, Schoonjans K, Albrechtsen R, Gillum MP, et al. Bile acids drive colonic secretion of glucagon-like-peptide 1 and peptide-YY in rodents. Am J Physiol Gastrointest Liver Physiol. 2019;316. G574-G84.
[46] Graham DS, Liu G, Arasteh A, Yin XM, Yan S. Ability of high fat diet to induce liver pathology correlates with the level of linoleic acid and Vitamin E in the diet. PLoS One. 2023;18:e0286726.
[47] Zhang Y, Xue R, Zhang Z, Yang X, Shi H. Palmitic and linoleic acids induce ER stress and apoptosis in hepatoma cells. Lipids Health Dis. 2012;11:1.
[48] Feldstein AE, Lopez R, Tamimi TA, Yerian L, Chung YM, Berk M, et al. Mass spectrometric profiling of oxidized lipid products in human nonalcoholic fatty liver disease and nonalcoholic steatohepatitis. J Lipid Res. 2010;51:3046–54.
[49] Kirovski G, Stevens AP, Czech B, Dettmer K, Weiss TS, Wild P, et al. Down-regulation of methylthioadenosine phosphorylase (MTAP) induces progression of hepatocellular carcinoma via accumulation of 5'-deoxy-5'-methylthioadenosine (MTA). Am J Pathol. 2011;178:1145–52.
[50] Czech B, Dettmer K, Valletta D, Saugspier M, Koch A, Stevens AP, et al. Expression and function of methylthioadenosine phosphorylase in chronic liver disease. PLoS One. 2013;8:e80703.
[51] Benz C, Angermuller S, Otto G, Sauer P, Stremmel W, Stiehl A. Effect of tauroursodeoxycholic acid on bile acid-induced apoptosis in primary human hepatocytes. Eur J Clin Invest. 2000;30:203–9.
[52] Liu N, Feng J, Lv Y, Liu Q, Deng J, Xia Y, et al. Role of bile acids in the diagnosis and progression of liver cirrhosis: a prospective observational study. Exp Ther Med. 2019;18:4058–66.
[53] Park KS, Sin PJ, Lee DH, Cha SK, Kim MJ, Kim NH, et al. Switching-on of serotonergic calcium signaling in activated hepatic stellate cells. World J Gastroenterol. 2011;17:164–73.
[54] Ebrahimkhani MR, Oakley F, Murphy LB, Mann J, Moles A, Perugorria MJ, et al. Stimulating healthy tissue regeneration by targeting the 5-HT(2)B receptor in chronic liver disease. Nat Med. 2011;17:1668–73.
[55] Ruddell RG, Oakley F, Hussain Z, Yeung I, Bryan-Lluka LJ, Ramm GA, et al. A role for serotonin (5-HT) in hepatic stellate cell function and liver fibrosis. Am J Pathol. 2006;169:861–76.
[56] Holst JJ. The incretin system in healthy humans: the role of GIP and GLP-1. Metabolism 2019;96:46–55.
[57] De Silva A, Bloom SR. Gut hormones and appetite control: a focus on PYY and GLP-1 as therapeutic targets in obesity. Gut Liver 2012;6:10–20.
[58] Martin C. The physiology of amylin and insulin: maintaining the balance between glucose secretion and glucose uptake. Diabetes Educ. 2006;32(Suppl. 3). 101S-4S.
[59] Skoracka K, Hryhorowicz S, Schulz P, Zawada A, Ratajczak-Pawlowska AE, Rychter AM, et al. The role of leptin and ghrelin in the regulation of appetite in obesity. Peptides 2025;186:171367.
[60] McTernan PG, Kusminski CM, Kumar S. Resistin. Curr Opin Lipidol. 2006;17:170–5.
[61] Mojiminiyi OA, Abdella NA. Associations of resistin with inflammation and insulin resistance in patients with type 2 diabetes mellitus. Scand J Clin Lab Invest. 2007;67:215–25.
[62] Bernsmeier C, Meyer-Gerspach AC, Blaser LS, Jeker L, Steinert RE, Heim MH, et al. Glucose-induced glucagon-like peptide 1 secretion is deficient in patients with non-alcoholic fatty liver disease. PLoS One. 2014;9:e87488.
[63] Wang F, Yoder SM, Yang Q, Kohan AB, Kindel TL, Wang J, et al. Chronic high-fat feeding increases GIP and GLP-1 secretion without altering body weight. Am J Physiol Gastrointest Liver Physiol. 2015;309:G807–15.
[64] Thomas C, Gioiello A, Noriega L, Strehle A, Oury J, Rizzo G, et al. TGR5-mediated bile acid sensing controls glucose homeostasis. Cell Metab. 2009;10:167–77.
[65] Brighton CA, Rievaj J, Kuhre RE, Glass LL, Schoonjans K, Holst JJ, et al. Bile acids trigger GLP-1 release predominantly by accessing basolaterally located G protein-coupled bile acid receptors. Endocrinology 2015;156:3961–70.
[66] Ye L, Mueller O, Bagwell J, Bagnat M, Liddle RA, Rawls JF. High fat diet induces microbiota-dependent silencing of enteroendocrine cells. Elife 2019:8.
[67] Yu XX, Qiu WL, Yang L, Li LC, Zhang YW, Xu CR. Dynamics of chromatin marks and the role of JMJD3 during pancreatic endocrine cell fate commitment. Development 2018:145.
[68] Li HJ, Ray SK, Kucukural A, Gradwohl G, Leiter AB. Reduced Neurog3 gene dosage shifts enteroendocrine progenitor towards goblet cell lineage in the mouse intestine. Cell Mol Gastroenterol Hepatol. 2021;11:433–48.
[69] Solorzano-Vargas RS, Bjerknes M, Wang J, Wu SV, Garcia-Careaga MG, Pitukcheewanont P, et al. Null mutations of NEUROG3 are associated with delayed-onset diabetes mellitus. JCI Insight. 2020:5.
[70] Tan S, Santolaya JL, Wright TF, Liu Q, Fujikawa T, Chi S, et al. Interaction between the gut microbiota and colonic enteroendocrine cells regulates host metabolism. Nat Metab. 2024;6:1076–91.
[71] You D, Nilsson E, Tenen DE, Lyubetskaya A, Lo JC, Jiang R, et al. Dnmt3a is an epigenetic mediator of adipose insulin resistance. Elife 2017:6.
[72] Tamilwanan S, Aziz Z, Rong LY, Bitar AN, Zarzour RHA, Alshehade SA. Efficacy of GLP-1 receptor agonists and dual GLP-1/GIP receptor agonists in managing MALFD: a meta-analysis of randomized controlled trials. BMC Gastroenterol. 2025;25:765.
[73] Lai J, Luo L, Zhou T, Feng X, Ye J, Zhong B. Alterations in circulating bile acids in metabolic dysfunction-associated steatotic liver disease: a systematic review and meta-analysis. Biomolecules 2023:13.
[74] Puri P, Daita K, Joyce A, Mirshahi F, Santhekadur PK, Cazanave S, et al. The presence and severity of nonalcoholic steatohepatitis is associated with specific changes in circulating bile acids. Hepatology 2018;67:534–48.
[75] Gillard J, Clerbaux LA, Nachit M, Sempoux C, Staels B, Bindels LB, et al. Bile acids contribute to the development of non-alcoholic steatohepatitis in mice. JHEP Rep. 2022;4:100387.
[76] Wouters K, van Gorp PJ, Bieghs V, Gijbels MJ, Duimel H, Lutjohann D, et al. Dietary cholesterol, rather than liver steatosis, leads to hepatic inflammation in hyperlipidemic mouse models of nonalcoholic steatohepatitis. Hepatology 2008;48:474–86.
[77] Ichimura-Shimizu M, Watanabe S, Kashirajima Y, Nagatomo A, Wada H, Tsuneyama K, et al. Dietary cholic acid exacerbates liver fibrosis in NASH model of Sprague-Dawley rats fed a high-fat and high-cholesterol diet. Int J Mol Sci. 2022;23.
[78] Lyu S, Yang J, Xin X, Sun Q, Cai B, Wang X, et al. Characteristics of serum bile acid profiles among individuals with metabolic dysfunction-associated steatotic liver disease. BMC Gastroenterol. 2025;25:334.
[79] Boursier J, Mueller O, Barret M, Machado M, Fizanne L, Araujo-Perez F, et al. The severity of nonalcoholic fatty liver disease is associated with gut dysbiosis and shift in the metabolic function of the gut microbiota. Hepatology 2016;63:764–75.
[80] Loomba R, Seguritan V, Li W, Long T, Klitgord N, Bhatt A, et al. Gut microbiome-based metagenomic signature for non-invasive detection of advanced fibrosis in human nonalcoholic fatty liver disease. Cell Metab. 2017;25(1054–62):e5.
[81] Zhang X, Chen J, van Kleef LA, Medina-Gomez C, van Meurs JBJ, Ikram MA, et al. Integrating gut microbiome and metabolome to gain insight into metabolic dysfunction-associated steatotic liver disease. Gastro Hep Adv. 2025;4:100783.
[82] Tolhurst G, Heffron H, Lam YS, Parker HE, Habib AM, Diakogiannaki E, et al. Short-chain fatty acids stimulate glucagon-like peptide-1 secretion via the G-protein-coupled receptor FFAR2. Diabetes 2012;61:364–71.
[83] Raza S, Rajak S, Yen PM, Sinha RA. Autophagy and hepatic lipid metabolism: mechanistic insight and therapeutic potential for MASLD. NPJ Metab Health Dis. 2024;2:19.
[84] Jornayvaz FR, Shulman GI. Diacylglycerol activation of protein kinase Cepsilon and hepatic insulin resistance. Cell Metab. 2012;15:574–84.
[85] Iturbe-Rey S, Maccali C, Arrese M, Aspichueta P, Oliveira CP, Castro RE, et al. Lipotoxicity-driven metabolic dysfunction-associated steatotic liver disease (MASLD). Atherosclerosis 2025;400:119053.
[86] Li S, Gao D, Jiang Y. Function, detection and alteration of acylcarnitine metabolism in hepatocellular carcinoma. Metabolites 2019:9.
[87] Carli F, Della Pepa G, Sabatini S, Vidal Puig A, Gastaldelli A. Lipid metabolism in MASLD and MASH: from mechanism to the clinic. JHEP Rep. 2024;6:101185.
[88] Older EA, Zhang J, Ferris ZE, Xue D, Zhong Z, Mitchell MK, et al. Biosynthetic enzyme analysis identifies a protective role for TLR4-acting gut microbial sulfonolipids in inflammatory bowel disease. Nat Commun. 2024;15:9371.

[89] Modasia A, Parker A, Jones E, Stentz R, Brion A, Goldson A, et al. Regulation of enteroendocrine cell networks by the major human gut symbiont Bacteroides thetaiotaomicron. Front Microbiol. 2020;11:575595.
[90] Yano JM, Yu K, Donaldson GP, Shastri GG, Ann P, Ma L, et al. Indigenous bacteria from the gut microbiota regulate host serotonin biosynthesis. Cell 2015;161:264–76.
[91] Alsudayri A, Perelman S, Brewer M, Chura A, McDevitt M, Drerup C, et al. Gut microbiota regulate maturation and mitochondrial function of the nutrient-sensing enteroendocrine cell. Development 2024:151.